THESIS FOR THE DEGREE OF LICENTIATE OF ENGINEERING

Analysis of Power Performance and Mooring Fatigue Damage for Wave Energy Parks

XINYUAN SHAO

Analysis of Power Performance and Mooring Fatigue Damage for Wave Energy Parks

XINYUAN SHAO

Analysis of Power Performance and Mooring Fatigue Damage for Wave Energy Parks

XINYUAN SHAO
Chalmers University of Technology
Department of Mechanics and Maritime Sciences
Division of Marine Technology

Abstract

Wave energy has been recognized as a promising alternative to traditional energy sources due to its cleanliness and sustainability. To harness this energy, wave energy converters (WECs) are utilized. These WECs operate using a variety of working principles and are typically deployed in large numbers in the form of wave energy parks to generate electricity with high efficiency and low levelized cost of energy (LCOE). However, the interaction effects between multiple WECs can positively or negatively impact power performance and mooring fatigue damage, highlighting the importance of numerical methodologies to evaluate such effects and facilitate agile wave energy park design processes.

The primary objective of this thesis was to develop numerical methodologies and data post-processing techniques to effectively access single WECs and wave energy parks consisting of two different WEC concepts belonging to the point absorber group: WaveEL and NoviOcean. Specifically, two methodologies were built based on the potential theory and a computational fluid dynamics (CFD) method, for which the boundary element method (BEM) and direct numerical simulation (DNS) with volume of fluid (VOF) modelling were adopted, respectively. These methods were implemented using the software, DNV SESAM and STAR-CCM+. The WEC concepts were evaluated in terms of the performance and mooring fatigue damages of each WEC concept with varying WEC generations, wave conditions, wave incoming directions and wave park layouts.

This thesis contributes to a better understanding of WEC system modelling, power performance and mooring fatigue damage estimation. Ultimately, these findings are anticipated to facilitate the development of optimized wave energy park layouts in the future.

Keywords: CFD, mooring fatigue, potential theory, power output, SESAM, STAR-CCM+, wave energy park, WEC.

Preface

This thesis consists of the research work carried out at the Division of Marine Technology, Department of Mechanics and Maritime Sciences at Chalmers University of Technology during the years 2021 – 2023. Financial support for this research was provided by the project 'INTERACT – Analysis of array systems of wave energy converter with regard to interaction effects in the LCOE and fatigue analyses', which is funded by the Swedish Energy Agency under grant agreement 2019-026869 and the project 'Control of wave energy converters based on wave measurements, for optimal energy absorption (WAVEMEASURE)', funded by the Swedish Energy Agency under the grant agreement 50197-1.

Time flies faster than I ever could have imagined. Looking back on the past two years, I have grown so much with the help and love of so many people, and I am so grateful for it.

I want to sincerely thank Professor Jonas Ringsberg, Associate Professor Hua-Dong Yao, Adjunct Professor Erland Johnson and Associate Professor Zhiyuan Li for their unwavering support throughout my study. Thank you, Assistant Professor Shun-Han Yang, for guiding my early research.

I am deeply thankful for all my colleagues at the Division of Marine Technology. Thank you for believing in me and trusting me to represent you in the PhD council. Let's work together to make our division an even more joyful workplace.

I want to thank my friend Yao Cai. Every lunchtime becomes so enjoyable with you. Your friendship has been a true blessing in my life. Also, special thanks and love to Yao's cat Lyapunov for waking me up at 6 am during the thesis writing phase.

I also want to thank my parents and siblings. I would never have made it this far without your support and love.

Finally, I want to thank myself for the dedication and hard work I have put into completing this thesis.

Xinyuan Shao 邵欣圆
Gothenburg, April 2023

Contents

List of appended papers

Paper I X. Shao, H.-D. Yao, J.W. Ringsberg, Z. Li, E. Johnson, G. Fredrikson. (2022). *A comparison of the performance and characteristics of two generations Waves4Power WaveEL wave energy converters.* Eds: C. Guedes Soares. Trends in Renewable Energies Offshore - Proceedings of the 5th International Conference on Renewable Energies Offshore (RENEW 2022), 8-10 November 2022, Lisbon, Portugal, p. 277-284, DOI: 10.1201/9781003360773.

Paper II X. Shao, H.-D. Yao, J.W. Ringsberg, Z. Li, E. Johnson. (2023). *Performance analysis of two generations of heaving point absorber WECs in farms of hexagon-shaped array layouts.* Submitted to Journal of Ships and Offshore Structures (under review).

Paper III X. Shao, J.W. Ringsberg, H.-D. Yao, Z. Li, E. Johnson. (2023). *Fatigue of mooring lines in wave energy parks.* Eds: J. W. Ringsberg, C. Guedes Soares, Advances in the Analysis and Design of Marine Structures - Proceedings of the 9th International Conference on Marine Structures (MARSTRUCT 2023): 3-5 April 2023, Gothenburg, Sweden, p. 205-211, DOI: 10.1201/9781003399759.

Paper IV X. Shao, H.-D. Yao, J.W. Ringsberg, J. Skjöldhammer, J. Lin. (2023). *FSI simulation and analyses of a non-resonant buoyant wave energy converter.* Proceedings of the 42nd International Conference on Ocean, Offshore and Arctic Engineering (OMAE 2023): 11-16 June 2023, Melbourne, Australia, paper no. OMAE2023-101335.

List of other published papers by the author

Paper A   X. Shao, M. C. Santasmass, X. Xue, J. Niu, L. Davidson, A. J. Revell, H. - D Yao. (2022). *Near-wall modelling of forests for atmosphere boundary layers using lattice Boltzmann method on GPU*. Engineering Application of Computational Fluid Mechanics, 16:1, 2143-2156, DOI: 10.1080/19942060.2022.2132420.

x

Nomenclature

Greek notations

ϕ	Velocity potential [m²/s]
ρ	Density [kg/m³]
ζ	Wave elevation [m]
ω	Wave frequency [rad/s]
η	Hydrodynamic efficiency [-]
ξ	Heave motion [m]

Latin notations

$A(\omega)$	Frequency dependent added mass [kg]
B_{PTO}	Power take-off damping [kNs/m]
$C(\omega)$	Frequency dependent added damping [kNs/m]
D	Mooring line damage [-]
D_1	Linear damping [kNs/m]
D_2	Quadratic damping [kNs²/m²]
D_{WEC}	Wave energy converter width
$F_{excitation}$	Wave excitation force [N]
$F_{moorings}$	Mooring force [N]
F_{PTO}	Power take-off force [N]
$F_{radiation}$	Radiation force [N]
$F_{restore}$	Restoring force [N]
g	Gravity [m/s²]
h	Averaged water depth [m]
k	Wave number [1/m]
K	Hydrostatic stiffness
$\vec{n}$	Normal vector of body surfaces [-]
p	Pressure [Pa]
p_0	Atmospheric pressure [Pa]
P	Power output [W]
q	Excitation force [N]
R_i	Relative tension cycle [-]
t	Time [s]
T_{sim}	Simulated physical time

$\vec{U}$	Body velocity [m/s]
$\vec{V}$	Velocity [m/s]

Abbreviations

BEM	Boundary Element Method
CFD	Computational Fluid Dynamics
COG	Centre Of Gravity
DNS	Direct Numerical Simulation
FEM	Finite Element Method
LCOE	Levelized Cost Of Energy
LP	Linear Potential
N-S	Navier-Stokes
OWC	Oscillating Water Column
PDE	Partial Differential Equation
PTO	Power Take-Off
RFC	Rainflow Count
RN	Relative Tension-Number of Cycles to Failure
VOF	Volume Of Fluid
WEC	Wave Energy Converter

1 Introduction

Wave energy is a renewable energy source that has attracted increasing attention due to its abundant reserves and high energy density. Wave energy converters (WECs) are taking centre stage in the harvest of wave energy from the ocean. However, a single WEC usually cannot provide a sufficient amount of electricity with low levelized cost of energy (LCOE). Therefore, multiple WECs should be deployed in the form of wave energy parks (also called wave parks, wave farms, wave energy farms, or WEC arrays) to achieve a cost-efficient, commercial wave energy market solution. This thesis focuses on the numerical simulation of single WECs and wave parks to analyse their power performance and fatigue damage of mooring lines under the influence of interaction effects. The following sections introduce the background, motivation, and objectives of this thesis.

1.1 Background and motivation

Wave, solar, and wind energy are three promising sources of renewable energy. Wind energy originates from air movement due to uneven heating by the sun, while wave energy is generated from winds blowing across the surface of the ocean. During this process, in which solar energy is converted to wind energy and then wave energy, the energy intensity increases from 0.1–0.3 kW/m^2 on the horizontal surface of the earth to 0.5 kW/m^2 perpendicular to wind direction, then to 2–3 kW/m^2 perpendicular to incoming wave direction (Falnes, 2007). Wave energy can travel farther with less energy loss than wind power. Additionally, unlike solar energy, wave energy can offer power around the clock. Wave energy also has great potential to provide power at sea to support various offshore activities and fulfil the energy needs of rural coastal communities (LiVecchi et al., 2019). These advantages have contributed to making wave energy a rising star in the renewable energy market.

Wave energy extraction has a long history that dates back to 1799, when Pierre-Simon and his son filed the first patent regarding the technology in Paris. The development of wave energy extraction has continued since then; a rise in studies on WECs started in the 1970s in the context of increasing oil prices caused by the oil crisis. However, interest in the topic stagnated in the 1980s when oil prices dropped, thereby limiting funding for wave energy. In 1994, wave energy returned to centre stage with the help of the Fourth Framework Programme of the European Community (Polinder and Scuotto, 2005). Since then, in countries with abundant wave energy resources, such as Sweden, Denmark, Norway, Portugal, Ireland and the United Kingdom, wave energy has been considered a viable energy source, and wave energy extraction technologies have been under development with governmental support for many years (Clément et al., 2002).

WECs can be categorized by different styles. The most well-known WEC classification was created by Falcão (2010), stating that the WECs can be classified as oscillating water column (OWC), oscillating bodies or overtopping devices based on working principles. Each sub-category can be further divided into floating, fixed or submerged structures based on the mobility of the devices. The details of these categorizations can be found in Figure 1 and Figure 2. It is worth noting that even though they may use different working principles, the different categories of WECs share the ultimate goal of transferring wave energy into electricity with higher efficiency and larger output while achieving lower investment and maintenance costs.
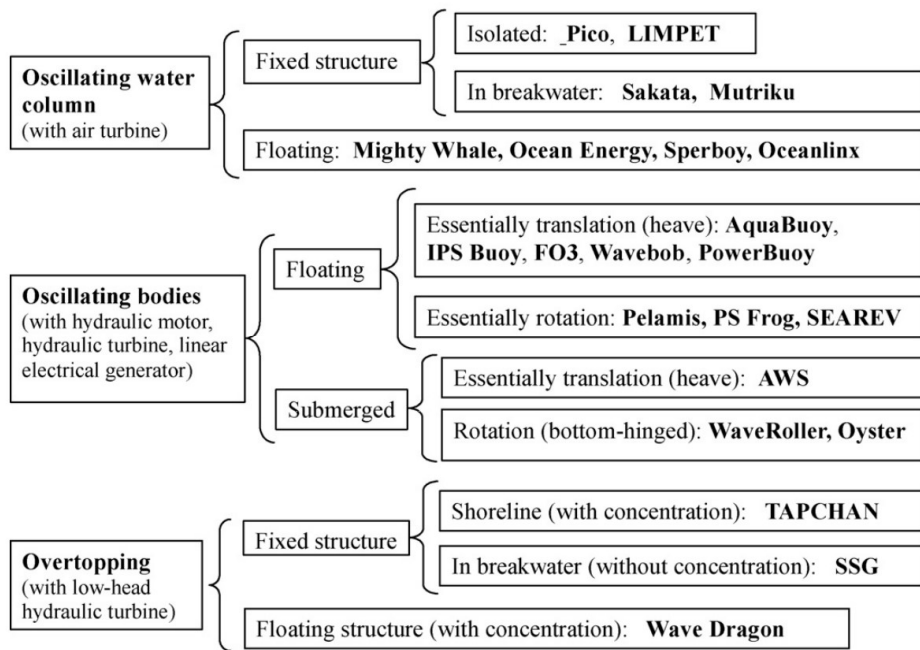
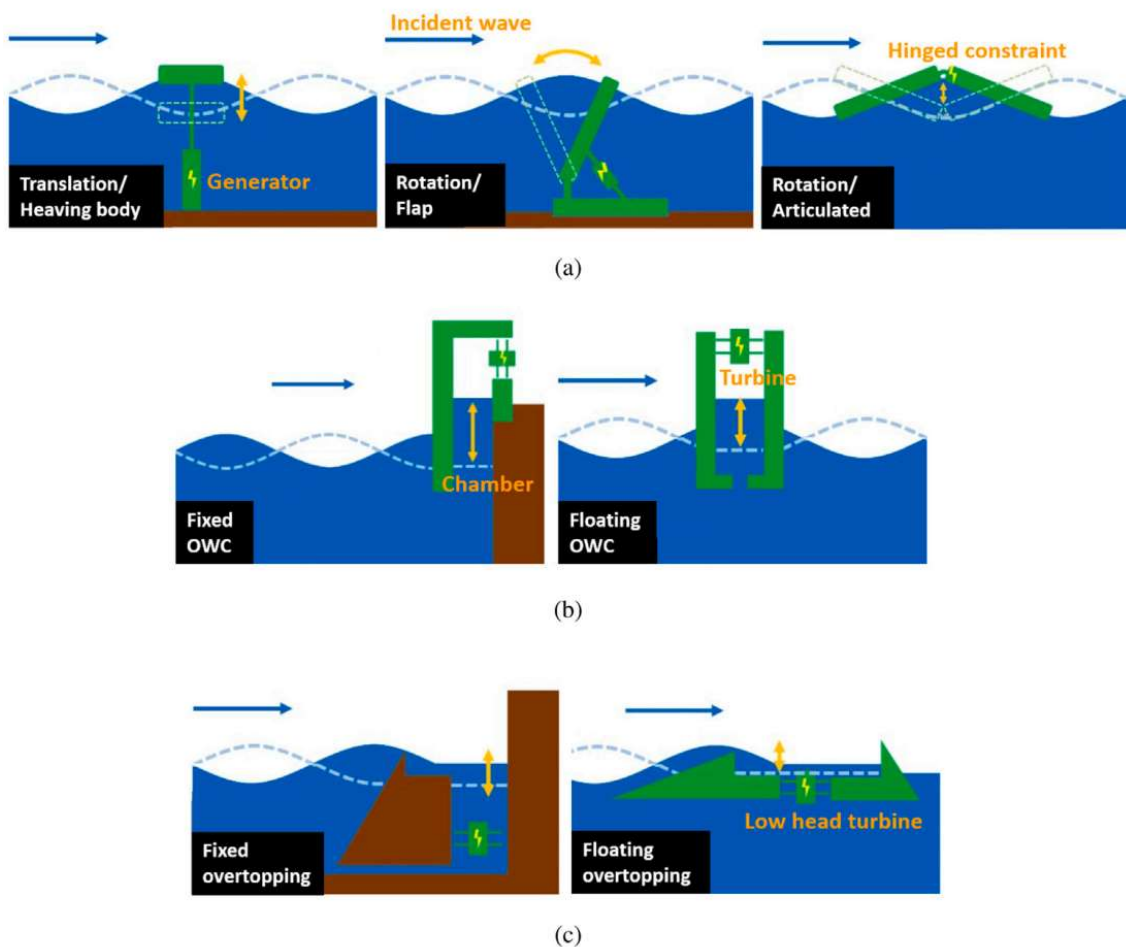Figure 1. WEC classification (Falcão, 2010).

Figure 2. Schematic diagrams of WEC according to working principles: (a) oscillating body, (b) OWC, and (c) overtopping device (Jin and Greaves, 2021).

Interaction effects in wave parks

There is a consensus that WECs should be deployed in large numbers in the form of wave parks so that total and averaged power output can be maximized as compared to a single WEC and LCOE can be minimized. It is believed that this format allows for large-scale commercialization. However, the overall evaluation of a wave park is not as simple as '1+1=2'. A single WEC induces diffracted waves due to the block effect of the WEC and radiated waves due to the oscillation of the WEC. In a wave park where multiple WECs exist in a relatively close proximity, the diffracted and radiated waves from different WECs interfere with each other, resulting in complex wave fields, as shown in Figure 3. These interferences are called interaction effects. Unlike interaction effects in the wind energy field, which only alter wind field for downwind turbines (González-Longatt et al., 2012), wave interaction effects can propagate within the entire water field, affecting all WECs.
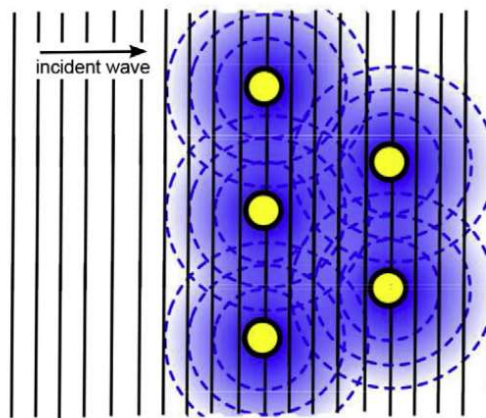

Figure 3. The interfered wave field caused by interaction effects (Babarit, 2013).

The changes in the wave field due to interaction effects cause changes in wave excitation force, consequently affecting the motion of WECs. Radiation force, which occurs due to the oscillating motion of WECs, is changed accordingly, in addition to the restoring force and forces from the power take-off (PTO) and the moorings. Moreover, as the motion of the WECs is affected, power output is changed as well. In the pioneering works by Budal (1977) and Falnes (1980), the authors' analytical solutions show that the interaction effects inside WEC arrays could either be constructive or destructive to power output depending on wave conditions and array layouts. There are also some counterintuitive findings regarding the interaction effect in wave parks. For example, Babarit (2010) showed that the interaction effects on the wave excitation force are larger for the first body, which is the first body to face incoming waves, than the second body, which is thought to be in a disturbed field. These findings point out the uncertainty and complexity in wave park design and power output estimation processes.

It has also been confirmed by various experiments that the interaction effects influence power output performance. Stallard et al. (2008) experimented with three array layouts, three WECs in attenuator configuration, nine WECs in square arrangement and an array of 3 × 4 WECs, finding that the interactions between closely spaced WECs affected power output performance either positively or destructively. Experimental results from Weller et al. (2010) of a small, two-dimensional 12-WEC (four rows relative to the wave

direction) array showed that the power output of the fourth row was impaired significantly by the interaction effects.

Interaction effects do not only influence power output performance. Krivtsov and Linfoot (2014) demonstrated that the extreme peak mooring loads in the leading mooring line of a 5-WEC array were almost doubled during their experiment compared with those of a single WEC in similar environment conditions. Such mooring failure by fatigue damage is added to the maintenance costs, and as such, fatigue damage should also be considered in the design of wave parks.

Due to the high cost of physical experiments, numerical methods are more popular for designing wave parks and evaluating existing wave park designs. In the early period of interaction studies, analytical methods were popular. The importance of interaction effects was brought to attention by analytical solutions of simplified WEC arrays developed by Budal (1977) and Falnes (1980). However, these are not suitable for the WECs currently under development because they do not consider multiple degrees of freedom of WECs and large-scale WEC arrays. Two representative and practical numerical methods for simulating wave parks are the boundary element method (BEM) (also known as the panel method) and the computational fluid dynamic (CFD) method. Using linear assumptions and potential theory, BEM calculates hydrodynamic coefficients, such as added mass and added damping in the frequency domain, while CFD considers viscous, turbulent, and non-linear effects important in extreme sea conditions. Explanations of the two methods are provided in Chapter 2.

Many case studies have used the two methods to successfully assess interaction effects. Balitsky et al. (2017) coupled a BEM solver and a wave propagation model to study the effect of separation distance on the power output performance of a wave park. Devolder et al. (2018) adapted the open-source CFD software OpenFoam to investigate 2-, 5- and 9-WEC arrays, with their simulation results showing good agreement with experimental results. Lee et al. (2018) studied the interactions between a floating offshore wind turbine platform and multiple WECs using the BEM solver WAMIT. Yang et al. (2020a) simulated WEC arrays using the commercial DNV SESAM software package based on potential theory, finding that the effects of interaction on the averaged power of a 10-WEC array ranged from -17% to +23% depending on the incident wave direction. They also found that the fatigue damage could vary by more than tenfold due to the interaction effects. Poguluri et al. (2021) used BEM and CFD to simulate multiple WEC rotors, with the results showing strong agreement on pitch response and the q-factor quantifying the interaction effects between WECs. Li et al. (2022) coupled the CFD solver OpenFOAM and the multibody interaction solver MBDyn to simulate a mechanically connected WEC array.

This thesis addresses two WEC concepts from the companies Waves4Power and Novige, which can both be categorized as oscillating body devices that take advantage of heaving motion (heaving point absorbers). The following sections introduce each concept, respectively.

Waves4Power

The WaveEL WEC by Waves4Power was successfully tested at full scale in 2016. The essential components of the WaveEL buoy are shown in Figure 4. The concept functions

4

in the following manner: when buoy A moves following the coming waves, the water column inside the acceleration tube B also oscillates, which drives the water piston C. The water piston C is connected with the cassette D which contains the PTO system made of a hydraulic cylinder, accumulators, a hydraulic motor and a generator.
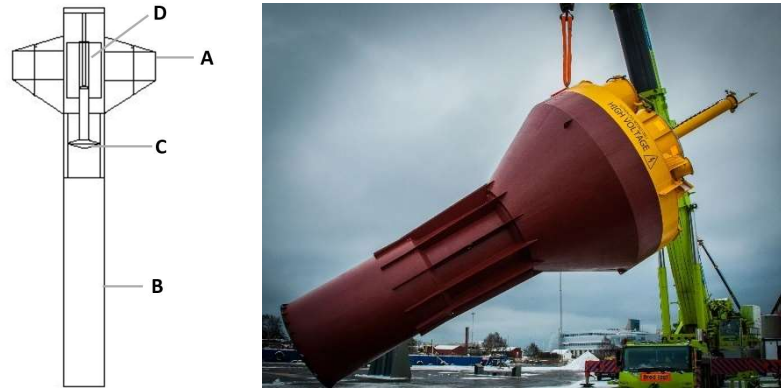

Figure 4. Left: components of WaveEL buoy (Waves4Power, 2021). Right: WaveEL in transportation (Stensvold, 2017).

Novige

Novige offers a unique WEC, dubbed NoviOcean, which is a non-resonant WEC that extracts energy from heaving motion. A non-resonant WEC has a higher resonant period than the wave periods. The NoviOcean WEC contains two parts: a rectangular floater and an inverted hydropower plant PTO system (Novige, 2023b). As shown in Figure 5, the PTO system consists of two components: the water turbine on top of the rectangular floater and a hydraulic cylinder under the water surface. The pressurized water pumped by the hydraulic cylinder flushes the water turbine to produce electricity.

Figure 5. Components of NoviOcean WEC (Novige, 2023a): the water turbine in the blue dashed box and the hydraulic cylinder in the white dash box.

The concepts from the two companies mentioned above use different working principles and PTO systems. They are discussed here not to prove which is the best, as it is believed that both of them are well-designed and can be deployed in proper locations successfully. Rather, they are introduced here because, as put by Falnes (2007): 'We should avoid re-inventing old inventions and repeating old mistakes. One mistake could be to believe my invention is the best one. Instead, we need to co-operate and work together'. That is, here they are discussed in order to compare them and provide opportunities for mutual learning and improvement.

1.2 Objective

There are many challenges hindering the repaid development of wave parks. WECs have different working principles, which makes their modelling vary by different concepts. Physical, on-site tests of wave parks are expensive and time-consuming, which makes it hard to obtain data that can guide wave park design. The influence of interaction effects on power performance and mooring fatigue damage requires careful evaluation using proper numerical methods.

The main objective of this thesis is to develop a methodology that covers the modelling, power output calculation and mooring fatigue damage evaluation for single WECs and WEC arrays. This methodology should be comprehensive and capable of covering a variety of WEC concepts, such as resonant and non-resonant point absorbers, and a variety of wave park designs.

The main objective of this thesis can thus be divided into several goals:

(i)   Propose methodologies for different WEC concepts to model their characteristics with acceptable accuracy for specific purposes. These methodologies should cover the whole system of single WECs and WEC arrays, including the PTO and mooring systems.

(ii)   Investigate the interaction effects of different WEC arrays with different WEC concepts. Systematically evaluate the data concerning power output performance and mooring fatigue damage.

(iii)   Compare different modelling methodologies and specify their applicable range.

1.3 Thesis outline

The outline of this thesis is as follows: Chapter 2 describes the methods, software, developed numerical models, and assumptions and limitations applied in this study. Chapter 3 summarizes the representative results from appended Papers I-IV. The conclusions of this thesis are presented in Chapter 0, followed by recommendations for future studies.

2 Methodology and numerical models

This chapter introduces the methodology and numerical models used in this thesis. The methodology section covers the potential theory method and CFD method, as well as some analytical methods for fatigue damage and power performance estimation. The software programs used are also introduced. The numerical models section contains explanations for WaveEL and NoviOcean models including their PTO and mooring system.

2.1 Methods and software

WECs are complex systems suffering sea loads, which include wave, current and wind load, PTO and mooring systems loads. When multiple WECs are implemented in a wave park, the interaction effects due to diffraction and radiation significantly affect the wave loads, and PTO and mooring loads are then affected as a consequence. There are two major methods of simulating wave loads exerted on a single WEC or a wave park: BEM, which is based on linear potential theory, and the CFD method, which is based on the mass conservation and Navier-Stokes (NS) equations.

BEM solves the Laplace equation with linearized boundary conditions in the frequency domain. Radiation force can then be obtained in the form of added mass and damping, while diffraction force is obtained in the form of wave excitation transfer functions. The equation of motion can also be solved in the frequency domain to obtain the response amplitude operators. One of the most representative BEM software programs is Wadam (Wadam, 2023). However, the frequency-domain method restricts it to a linear system. In order to include non-linear PTO and mooring forces, a time-domain method is necessary. The time domain analysis software used in this thesis was SIMA, which enables fully coupled analysis of marine systems and moorings (SIMA, 2023).

The CFD method can use direct numerical simulation (DNS) to solve the N-S equation with viscosity and instantaneous wet surface, making it more accurate under some circumstances. The STAR-CCM+ is a commercial CFD software that can use the volume of fluid (VOF) method to solve free-surface waves and the overset mesh approach to capture large body motions. The overset mesh approach enables fine mesh quality around the moving body, which is required for the accurate prediction of nonlinear hydrodynamic forces.

The two most interesting aspects of single WECs and wave parks are power performance and mooring line fatigue damage, which are crucial for LCOE calculation. Here, in-house Matlab codes were developed to calculate the power output and accumulated fatigue damage.

2.1.1 Loads on WECs

Current and wind loads may affect mooring axial forces by up to 60% (Ringsberg et al., 2020b). However, in this thesis, the current and wind loads were not considered. Thus, only the wave, PTO and mooring loads were included. According to Newton's second law of motion, the net force exerted on a body equals the product of its mass and acceleration:

$$F = m\ddot{x} \tag{1}$$

Regarding WECs under sea loads, Equation (1) can be written as:

$$m\ddot{x} = F_{excitation} + F_{radiation} + F_{restore} + F_{PTO} + F_{moorings} \qquad (2)$$

The right-hand side of Equation (2) should be evaluated. The definitions of each term are as follows:

(1) $F_{excitation}$ is the wave excitation force. This force is obtained by assuming that the WEC is restrained from any motions and that there are incident waves. This force can be divided into two parts: the first part is the force induced by the undisturbed wave called the Froude-Kriloff force. The second part is the diffraction force, which results from the changes to the wave field brought by the existence of the WEC.

(2) $F_{radiation}$ is the radiation force which is generated by oscillations of the WEC.

(3) $F_{restore}$ is generated by the change in buoyancy, which is proportional to the WEC motions.

(4) F_{PTO} is the force from the PTO system.

(5) $F_{moorings}$ is the station keeping force from the mooring system.

The excitation, radiation and restore forces are usually solved by the BEM in the frequency domain and then transferred to the time domain by inverse Fourier transform. The excitation force includes first-order force, which oscillates with the wave frequency, second-order wave drift force and higher-order ringing force. In this thesis, only the first-order excitation force was considered because the magnitude of high-order forces is relatively small compared to the first-order force. The first-order excitation force was calculated using the first-order wave force transfer function, which can be also obtained from the frequency domain analysis. Radiation force is usually identified as added mass and damping associated with WEC motions and velocities, respectively.

The PTO force is typically simplified as a force that relates to WEC motions and a damping coefficient. The modelling of PTO systems is introduced in detail in Section 2.2.3.

Mooring force is also relevant to the WEC motion and can be included in the system in a coupled or decoupled manner. The decoupled method computes mooring force and WEC motion in separate steps; that is, it first calculates the motion response at the fairleads of the WEC and then calculates mooring line responses based on the previous motion responses in the fairleads (Yang et al., 2016). In contrast, the coupled method solves the equations of motion of the WEC and its mooring system simultaneously so that the influence of the mooring lines on the WEC motions is also considered (Yang et al., 2016). It has been shown by Yang et al. (2016) that the coupled method is a better method of estimating the fatigue damage of mooring lines considering the accuracy and cost of computational resources. Therefore, in this thesis, only the coupled method was used. The specific methods for solving mooring force responses can use either the finite element method (FEM) or catenary analysis method. The latter does not include bending stiffness of moorings, while the former does and is typically used to provide a strong initial solution for finite element analysis (RIFLEX, 2019).

The interaction effects between multiple WECs directly result in diffraction and radiation force changes. As a consequence, the motion of the WEC is affected and the

force from PTO and the mooring system changes accordingly. The interaction effects on the diffraction force are described by each WEC's first-order wave force transfer function, while the radiation force interaction is covered by the coupled added mass and damping matrix.

2.1.2 Potential theory

Potential theory is the foundation for wave load calculation. Compared with the N-S equations, it has several assumptions that simplify computation; it assumes that the fluid is incompressible and inviscid, and that fluid motion is irrotational. Based on these assumptions, the fluid field can be described with a scalar velocity potential ϕ, a function of position vector $\vec{x} = (x, y, z)$ and time t. The velocity potential satisfies the Laplace equation:

$$\frac{\partial^2 \phi}{\partial x^2} + \frac{\partial^2 \phi}{\partial y^2} + \frac{\partial^2 \phi}{\partial z^2} = 0 \tag{3}$$

The Laplace equation can be solved with the BEM after implementing boundary conditions. Details of BEM can be found in Section 2.1.3.

After obtaining the velocity potential, the fluid velocity can be calculated as follows:

$$\vec{V} = \nabla \phi \tag{4}$$

Then the pressure p can be obtained using Bernoulli's equation:

$$p + \rho g z + \rho \frac{\partial \phi}{\partial t} + \frac{1}{2} \rho \vec{V} \cdot \vec{V} = C \tag{5}$$

where ρ is the density, z is the vertical position where $z = 0$ represents the mean free-surface level, and C is a constant.

The boundary conditions include the kinematic boundary conditions and the dynamic free-surface condition. The kinematic boundary conditions are that no fluid can penetrate the body surface and that the free surface will keep on the free surface. The dynamic free surface condition is that the water pressure equals the atmospheric pressure p_0. However, these two boundary conditions contain second-order terms and are applied over an unidentified position of the free surface, which make the solution of Equation (3) nonlinear and difficult to solve. Thus, the linear potential theory arises. The boundary conditions can be written as follows after linearization by ignoring second-order terms and applying the boundary conditions at equilibrium position. It should be noted that it is also assumed that there is no forward speed or current.

$$\frac{\partial \phi}{\partial n} = \vec{U} \cdot \vec{n} \text{ on body surface (kinematic body surface condition)} \tag{6}$$

$$\frac{\partial \zeta}{\partial t} = \frac{\partial \phi}{\partial z} \text{ on } z = 0 \text{ (kinematic free surface condition)} \tag{7}$$

$$g\zeta + \frac{\partial \phi}{\partial t} = 0 \text{ on } z = 0 \text{ (dynamic free surface condition)} \tag{8}$$

ζ is the wave elevation, $\vec{U}$ is the body velocity and $\vec{n}$ is the normal vector of the body surface. The detailed derivation can be found in Faltinsen (1993).

9

Note that assumptions of the linear potential theory come from two origins. First, the Laplace equation is derived from the N-S equation by assuming the fluid is incompressible and inviscid, and that fluid motion is irrotational. This assumption allows the fluid velocity vector to be described as a scalar velocity potential. Secondly, the boundary conditions are linearized based on the assumptions that the wavelength is much larger than the wave amplitude and the body dimensions. This linearization guarantees that the equation system is linear and the solution to the boundary value problem has a sinusoidal form.

Under the framework of linear potential theory, results in irregular waves can be calculated by summing up the results through a combination of regular waves. It is thus sufficient to analyse a body's motion response in regular waves with different frequencies and sum them up to get the body's motion response in irregular waves. Furthermore, similar to the force classification in Section 2.1.1, the velocity potential can also be separated as incident, diffraction and radiation potentials, which can be written as:

$$\phi = \phi_I + \phi_D + \phi_R \tag{9}$$

Each term fulfils the Laplace equation with specific boundary conditions, and ϕ_I represents the waves propagate without the body. It can be solved by combining Equations (3), (7) and (8) together with sea bottom boundary conditions. ϕ_D can be calculated by assuming fixed body and ϕ_D fulfils:

$$\frac{\partial \phi_I}{\partial n} + \frac{\partial \phi_D}{\partial n} = 0 \text{ on the body surface} \tag{10}$$

Finally, ϕ_R is solved by assuming no incident motion and that the body moves in one of the unconstrained degree-of-freedom (DoF). It is written as follows:

$$\phi_R = \sum_{i=1}^{N} \dot{\xi}_i \varphi_i \tag{11}$$

where $\dot{\xi}_i$ is the body velocity in mode i, and φ_i is the corresponding velocity potential of mode i with unit velocity.

The Froude-Kriloff, diffraction and radiation forces can be obtained by integrating pressure, which can be computed by adapting Equation (5) with the incident, diffraction and radiation potentials, respectively. Moreover, the radiation force can be divided into two parts: one part is proportional to the body velocity while the other one is proportional to the body acceleration. The coefficients of them are the added damping and mass, respectively.

The kinematic body surface condition should be applied to all the body surfaces for multiple bodies. The velocity potential is affected by the existence of multiple bodies and is how one body 'feels' the existence of other bodies nearby. The resulting interaction forces are diffraction force and radiation force.

2.1.3 Boundary element method (BEM)

BEM, also called the panel method, is a commonly used numerical method for solving velocity potential in which body surface is discretized into multiple panels (assuming the amount is N) and a source with unknown potential density is assigned to each panel. The total velocity potential can be obtained by summing up the distributed source. The source is carefully designed so that the Laplace equation and the free surface boundary conditions, as shown in Equations (7) and (8), are fulfilled. Obviously, the total velocity potential fulfils the Laplace equation and the free surface boundary conditions automatically. The last piece of the puzzle in solving the density of each source is satisfying the body boundary condition as shown in Equation (6) at each panel. A linear equation system with N equations and N unknowns can be obtained and solved. The establishment of proper source potentials is a complex mathematic process; more details can be found in Chapter 4 of Faltinsen (1993).

Due to the linear nature of the boundary value problem, BEM solves the velocity potential under regular waves with different frequency ω. Consequently, it can give the added mass, damping and wave excitation transfer function with varying frequencies, which are crucial for the time domain response analysis.

2.1.4 Equation of motion

Substituting the calculated added mass and damping, wave excitation force, PTO and mooring forces, etc. into Equation (2), according to SIMO (2019) for sinusoidal motion, the equation of motion can be written as:

$$(m + A(\omega))\ddot{x} + C(\omega)\dot{x} + D_1\dot{x} + D_2\dot{x}|\dot{x}| + K(x)x = q(t, x, \dot{x}) \tag{12}$$

where $A(\omega)$ is the frequency dependent added mass, $C(\omega)$ is the frequency dependent added damping, D_1 and D_2 are the linear and quadratic damping, $K(x)$ is the hydrostatic stiffness matrix and q is the excitation force.

Equation (12) can be solved in time domain by the convolution integral method. After an inverse Fourier transform, Equation (12) becomes:

$$(m + A(\omega=\infty))\ddot{x} + D_1\dot{x} + D_2\dot{x}|\dot{x}| + Kx + \int_0^t h(t-\tau)\dot{x}(\tau)d\tau = q(t, x, \dot{x}) \tag{13}$$

The retardation function can thus be written as:

$$h(\tau) = \frac{1}{2\pi}\int_{-\infty}^{\infty} C(\omega) + i\omega(A(\omega) - A(\omega=\infty))e^{i\omega t}d\omega \tag{14}$$

The added mass and added damping can be obtained from a boundary element solver. The excitation force includes the wave excitation force and other forces, such as mooring forces. The mooring force is evaluated in the time domain by some FEM software, such as RIFLEX, which is introduced in Section 2.1.8. The wave excitation force is obtained by the wave force transfer function provided by some boundary element solvers, such as Wadam, which is also introduced in Section 2.1.8. The PTO system can be represented in linear and quadratic damping terms. There are many methods of solving Equation (13), such as the Runge-Kutta method, for example (Runge, 1895).

2.1.5 Computational fluid dynamics (CFD)

In linear potential theory, viscous wave loads are discarded, and the free surface boundary conditions are applied to the mean water surface instead of the real-time water surface. These assumptions restrict the body motions and dimensions to relatively small sizes compared with the wavelength and wave amplitude, and viscosity can be ignored. However, the restrictions are not applicable to WECs with large motions or WECs working under harsh wave conditions.

The CFD method is a broad concept that refers to a method of solving a system of partial differential equations (PDEs) made of the N-S equation together with the continuity equation. One mathematical approach of the CFD method to solve the PDEs is the finite volume method, which uses the Gauss divergence theorem to express spatial partial derivatives as surface integrals (Mingham et al., 2016).

In this thesis, direct numerical simulations (DNS) solving an incompressible representation of the N-S equation, given that the flow contains limited turbulence. The volume of fluid (VOF) method (Ubbink, 1997) is used to compute the air/water interface. The overset mesh technique ensures that the refined mesh moves together with the WEC to capture the wave loads better.

The main advantages of the CFD model are that it applies the free surface boundary conditions to the real-time free surface instead of equilibrium water level, which enables the inclusion of nonlinearity and large WEC motions. Unlike the linear potential (LP) model, the CFD model also includes viscous forces.

2.1.6 Fatigue damage analysis of the mooring lines

Load cycle counting is the first step in fatigue analysis after obtaining a stress/strain history by either measurement or simulation. The most commonly used method is the rainflow count (RFC) method (Downing and Socie, 1982), for which there are available functions in Matlab. Accumulated fatigue damage is calculated by summing up the fatigue damage of each load cycle. Specifically, the relative tension number of cycles to failure (RN) approach should be applied for polyester mooring lines. The RN approach uses relative tension for rainflow counting. According to the position mooring standard (DNV, 2021), the mooring line damage D is calculated as follows:

$$D = \sum_i \frac{R_i^{\,m}}{\alpha} \cdot \gamma_D \qquad (15)$$

where i represents the i-th relative tension cycle identified by the RFC method. The parameters α and m are the intercept and slope of the RN curve. For the specific polyester mooring lines used in this study, these parameters are set to 0.259 and 13.46, respectively.

2.1.7 Power performance analysis

Power performance is relevant to the modelling approach of the PTO system in the numerical model. Although the PTO system is usually combined with control algorithms to maximise power output, this thesis does not include such control methods. Here, the PTO system is simplified as a linear damper. In this study, the value of the damping coefficient is either equal to the provided value given by the designer or equal to the added damping of the heave direction at the resonant frequency when the WEC is not

moored. This is because that damping value enables optimal power absorption (Alves, 2016). For PTO damping B_{PTO}, the power output is defined as follows:

$$P = \frac{1}{T_{sim}} \int_0^{T_{sim}} B_{\text{PTO}} [\dot{\xi}(t)]^2 dt \qquad (16)$$

where ξ is the translation in the heave direction (assuming heaving is the power extractive motion), and T_{sim} is the simulated physical time.

The hydrodynamic efficiency evaluates the capability of a WEC to extract energy from the waves. It is defined as:

$$\eta = \frac{\text{Power absorbed}}{\text{Power available within device width}} \qquad (17)$$

The available power within the device width is defined as:

$$P_{available} = \frac{\rho g^2 T H^2}{32\pi} \times D_{WEC} \qquad (18)$$

where T and H are wave height and period, D_{WEC} is the width of the WEC.

2.1.8 Software

The overall structure of the methods and the software are provided in Figure 6. Wadam and SIMA were the software programs used for the frequency domain and time domain analysis, respectively. Wadam is a software that calculates the wave-structure interaction problems for fixed or floating structures and solves 3D diffraction and radiation problems based on 3D potential theory solved by BEM in the frequency domain (Wadam, 2017). In this thesis, Wadam provides the added mass, the added damping and the first-order wave excitation force transfer function. SIMA is software used for marine operations and mooring analysis (SIMA, 2023). It has a variety of modules, but the two modules used in this thesis were SIMO and RIFLEX. SIMO computes the motions of floating structures under multiple loads (SIMO, 2019), while RIFLEX analyses flexible risers and other slender structures, such as mooring lines, fish cage systems and pipelines (RIFLEX, 2019). For WEC simulations, the two modules can be connected to make a coupled model so that the mooring line forces and WEC motions are calculated and included simultaneously, as mentioned in Section 0. The simulation pipeline 'Wadam + SIMA' was used in Papers I-IV.

STAR-CCM+ is a commercial CFD software developed by Siemens Digital Industries Software (STAR-CCM+, 2023). For WEC simulation, the free surface is captured by the VOF method, and the overset mesh technique is used to model the hydrodynamic force and WEC motions with high accuracy. The mooring and PTO loads can also be modelled as linear spring-dampers. STAR-CCM+ was used in Paper IV.

2.2 Numerical models

Although the two WEC concepts are both point absorbers that extract wave energy mainly from heaving motion, their working principles differ. This means that the modelling of each WEC should be treated separately, rather than rigidly casting two WECs into the same modelling pattern. Table 1 lists the models used in the papers; each model is introduced in detail in the following sections. It should be noted that Table 1

only provides an overview of the concepts. Their details can be found in the corresponding papers as listed in the last column of Table 1.

Additionally, it should be noted that the names of the models are different from those of the papers. Previously, the models were referred to by the software used, and therefore, they are called SIMA and STAR-CCM+ models in these papers. However, in this thesis, the models are denominated by the method they used. Therefore, the SIMA model is the linear potential theory model and the STAR-CCM+ model is the CFD model.
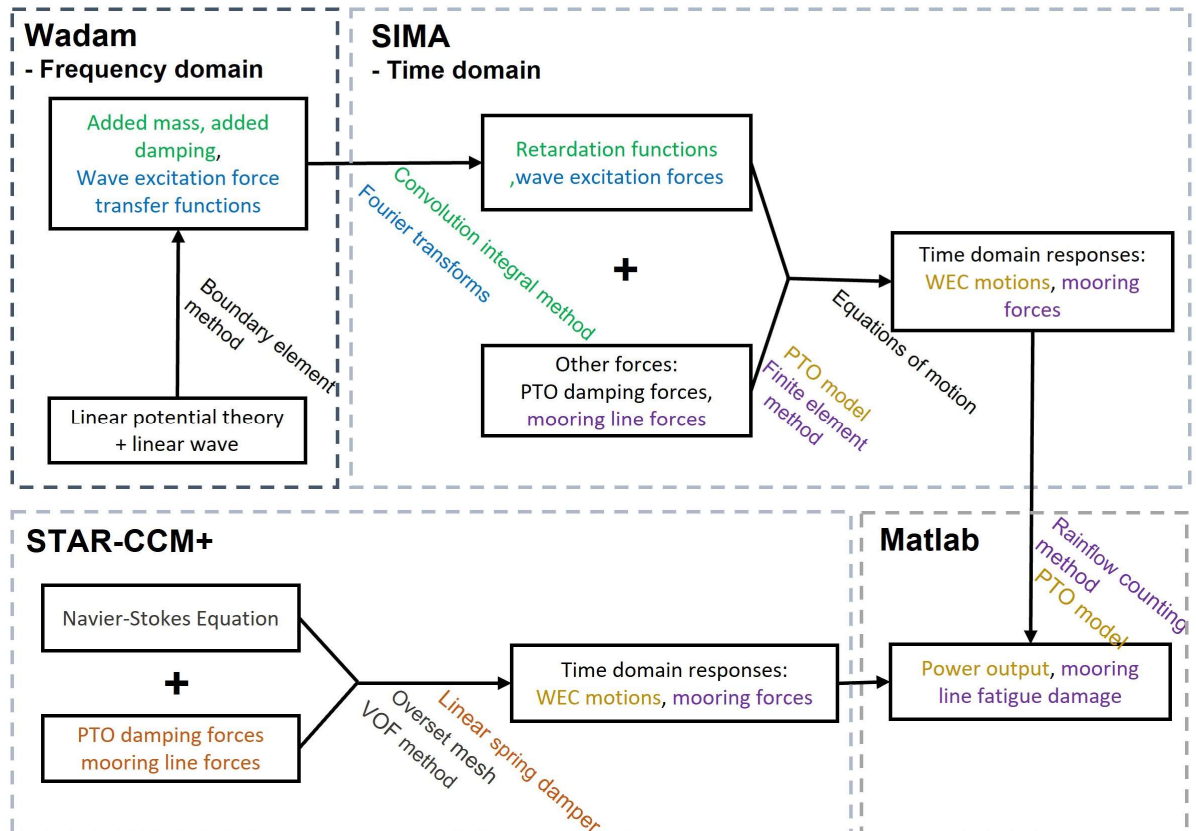
Figure 6. The overall structure of methods and software.

Table 1. Summary of the numerical models.

	WEC generation	Wadam	LP model (Single WEC)	LP model (WEC array)	CFD model (Single WEC)	Paper
W4P	WaveEL 3.0	x	x	6-WEC arrays	-	I, II & III
	WaveEL 4.0	x	x	6-WEC arrays	-	I, II & III
NoviOcean	-	x	x	2-WEC array	x	IV

2.2.1 W4P model - WaveEL

This section presents the single WEC model of WaveEL and three studied wave park configurations.

Single WEC

Waves4Power has proposed their newest generation, WaveEL 4.0, as a successor to the previous generation of WaveEL 3.0, which has been studied in the following works: Yang et al. (2016); Yang et al. (2017b); Yang et al. (2017a); Yang et al. (2018); Yang (2018); Yang et al. (2020a). WaveEL 4.0 has a different geometry from WaveEL 3.0. As shown in Figure 7 and Table 2, the length of the tube and the shape of the upper buoy differ, resulting in centre of gravity (COG) and the weight changes. These differences cause changes in the frequency-domain and time-domain responses, which are explained in Section 3.1.

In the mooring system (as shown in Figure 8), three mooring lines are spread out at angles of 120 degrees. Each mooring line contains two sections that are connected by a floater; section 1 denotes the mooring sections almost parallel to the still water level, while section 2 denotes the mooring sections nearly vertical to the seabed. Section 1 is always in tension, so that the horizontal motions are restrained, but the vertical motions are not limited as it is almost parallel to the water level. The properties of the mooring lines and floaters are explained in detail in Section 2.2.4.
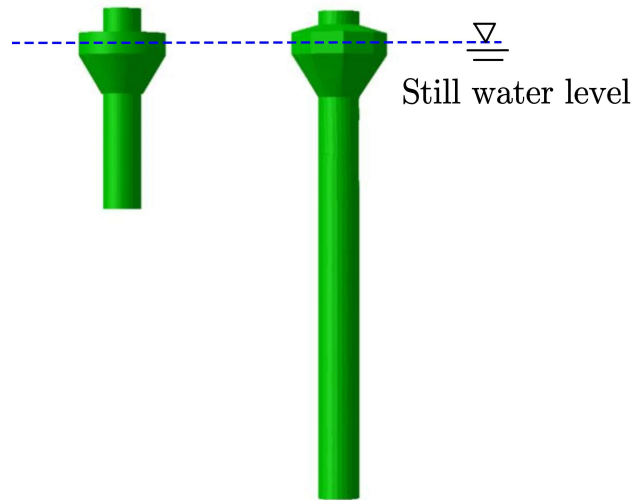

Figure 7. WaveEL 3.0 (left) and WaveEL 4.0 (right).

Table 2: Geometry parameters of the WEC concepts.

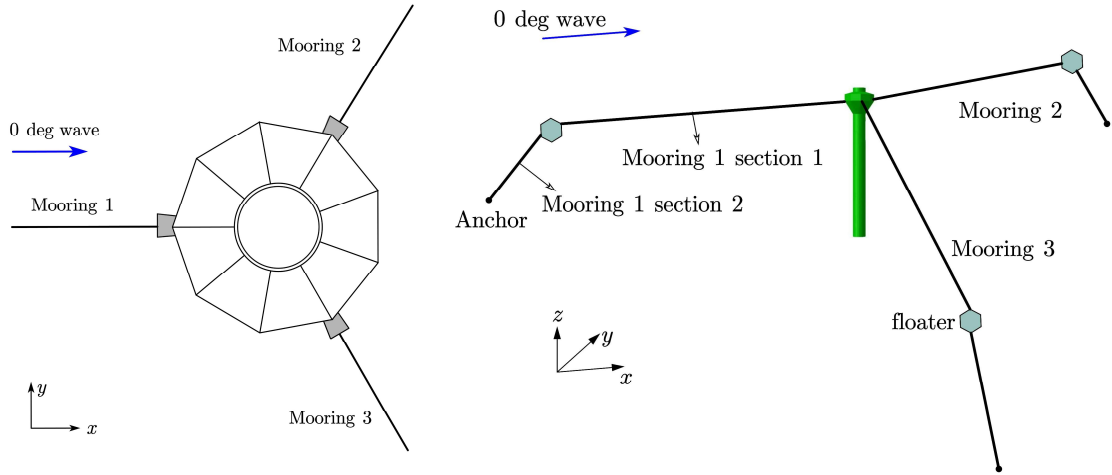|	WaveEL 3.0	WaveEL 4.0
COG [m] (origin at the mean water level)	-1.9	-10.6
Weight [ton]	140	217
Tube length [m]	10.7	37.1
Buoy diameter [m]	8	8.6
Tube outer diameter [m]	3.5	3.5

Figure 8. Mooring system: upper view (left) and iso view (right).

Wave parks

Three different layouts of wave parks, as shown in Figure 9 and Table 3, were studied. Hex1 and Hex2 are two types of 6-WEC wave park layouts proposed by Waves4Power, which differ in that all WECs in Hex1 share the central anchors, while in Hex2, the WEC only shares anchors with the two closest WECs. As such, Hex1 only needs seven anchors, while Hex2 needs twelve. Therefore, the cost of the mooring system of Hex1 is less than Hex2. However, as the WEC distance in Hex1 is smaller than Hex2, the possible negative interaction effects may result in lower power output of the whole wave park. StarBuoy is a 10-WEC wave park that is considered as one of the best designs under several criteria, such as LCOE, mooring fatigue life and power generation (Ringsberg et al., 2020a). Like Hex1, StarBuoy also shares a central anchor. From the dimension perspective, Hex1-80 is the most compact design, with a diameter of 139 m. Hex1-120 and StarBuoy share similar diameters of around 300 m. Hex2 has the largest diameter of 390 m due to its unshared anchors.

Table 3. Parameter of wave parks.

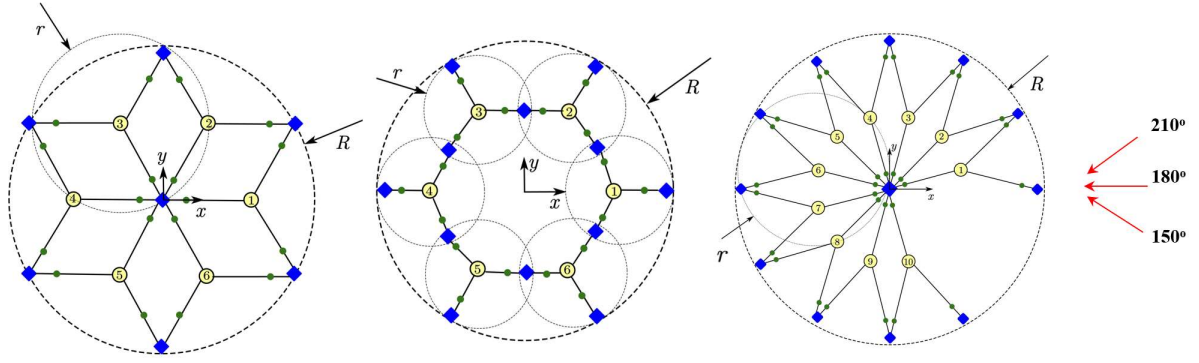| Wave parks	WEC distance [m]	R [m]	r [m]
Hex1-80 and Hex1-120: 6-WEC (sharing the centre anchor)	80; 120	139; 208	70; 104
Hex2: 6-WEC (not sharing the centre anchor)	260	390	130
StarBuoy: 10-WEC (Yang et al., 2020a)	52	200	100

Figure 9. Three wave park layouts. Yellow marks represent WECs, green marks represent floaters and blue squares represent anchors. From left to right: Hex1, Hex2 and StarBuoy.

2.2.2 NoviOcean model

In this section, the LP and CFD models for NoviOcean WEC are introduced. The LP models were developed for a single WEC and a 2-WEC array with different WEC orientations. Due to the lack of experimental data, validation of the LP model is not feasible at the moment. However, a CFD model of a single WEC was developed for verification comparisons with the LP model.

LP model – single WEC

The NoviOcean WEC system is shown in Figure 10, and general geometry information is given in Table 4. Like WaveEL, it also uses 2-section mooring lines. Four mooring lines with 90 degrees of separation pairs are deployed in the buoys' front and back. The PTO system, which contains a hydraulic cylinder and a central piston, is simplified as a spring-damper. Details can be found in Section 2.2.3.
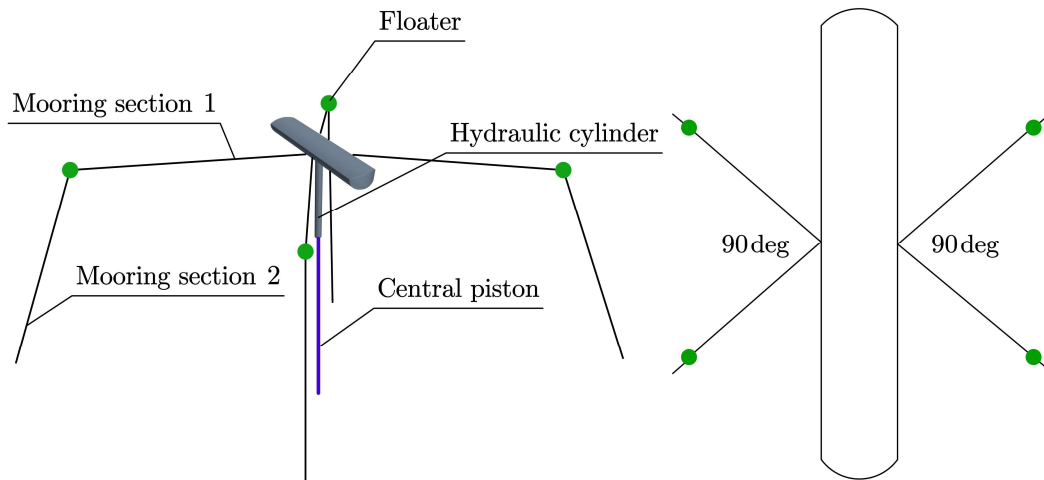

Figure 10. The NoviOcean model: the buoy, the mooring system and the central piston. The side view (left) and the top view (right).

17

Table 4. General information of NoviOcean WEC concept.

Property	Value
Length [m]	38.52
Width [m]	7.65
Height [m]	4.65
Mass [kg]	213000

LP model – 2-WEC wave park

Due to the non-axisymmetric feature of the NoviOcean WEC, two 2-WEC wave park layouts, as shown in Figure 11, were designed to study the interaction effects with varying distances and incoming wave directions. Case X and Case Y represent the orientation of the wave park layouts. The information on the simulated cases is listed in Table 5.
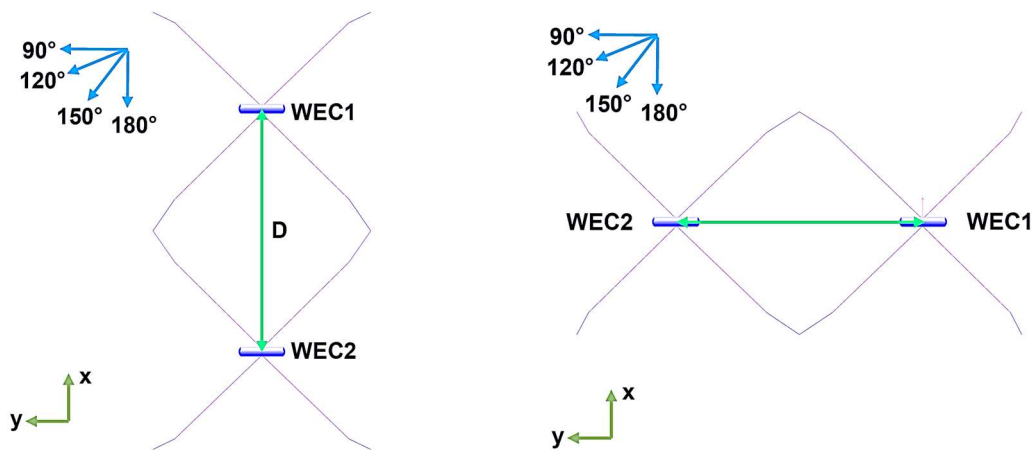

Figure 11. NoviOcean 2-WEC wave park layouts. Case X (left) and Case Y (right).

Table 5. Wave park simulation cases information.

Cases	WEC distance, D [m]	Wave incoming direction [degree]
Case X	200, 300, 400	90, 120, 150, 180
Case Y	200, 300, 400	90, 120, 150, 180

CFD model – single WEC

A CFD model for a single NoviOcean WEC was developed to verify the LP and CFD approaches. The CFD model is shown in Figure 12. It should be noted that section 2 of the mooring lines was not modelled due to the complexity of including floaters in STAR-CCM+. Instead, the ends of the first sections of the moorings were fixed at the position of the floater in still water conditions. A corresponding LP model without section 2 was developed to control variables in comparison. The model settings are listed and compared in Table 6.
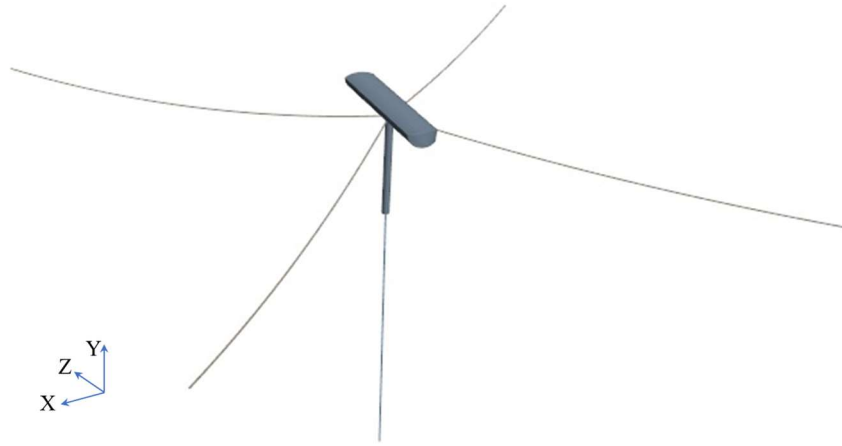
Figure 12. CFD model of a single NoviOcean WEC.

Table 6. LP and CFD model settings.

Property		LP	CFD
Wave	Wave theory	Linear	Linear
	Period [s]	9	9
	Height [m]	1.8	1.8
	Length [m]	126.5	126.5
Water depth		100	Deep water assumption
Buoy draft		1.25	1.25
Buoy DOFs		6 DOFs	X, Y, Z translations
Central piston	Stiffness [kN/m]	544	544
	Damping [kNs/m]	136	13
	Relaxation length [m]	73.5	73.5

2.2.3 PTO model

The PTO system of both WaveEL and NoviOcean were simplified as linear damping. The damping features are listed in Table 7. The power output calculation follows Equation (16).

Table 7. PTO system modelling.

WEC	PTO modelling	Properties
WaveEL	Linear damping	WaveEL 3.0: 40kN/m; WaveEL 4.0: 50 kN/m.
NoviOcean	Linear damping	See Table 6, central piston

2.2.4 Mooring line model

Although layouts of the mooring systems may differ between single-WEC concepts and wave parks, the material of the mooring line in this thesis is the same polyester line with

a diameter of 80 mm, unless otherwise specified. The mooring system modelling for each WEC model is summarised in Table 8. Note that the stiffness of the mooring line was a constant only in the single-WEC model for comparison with the CFD model. Other simulations adapted the non-linear stiffness feature as shown in Figure 13.

Table 8. Mooring system modelling parameters.

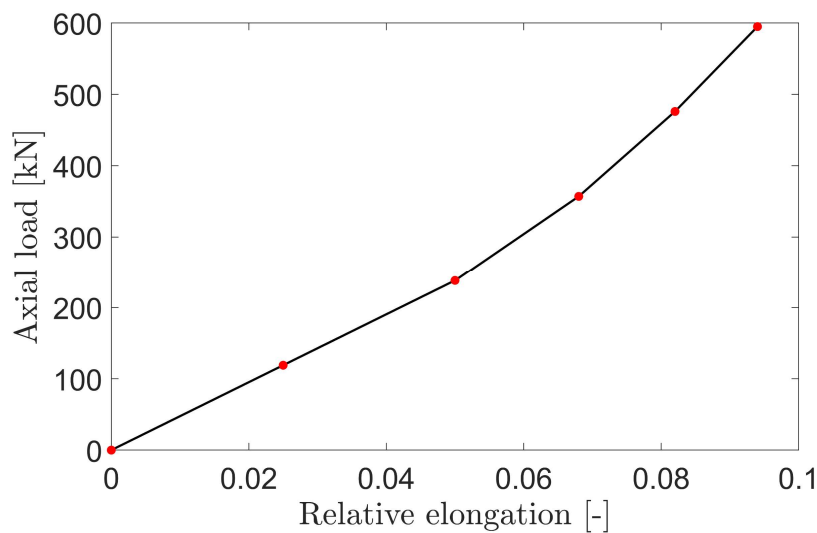| WEC	Mooring modelling	Sections	Floater fixing position	Mass	Material	Stiffness
WaveEL	Single WEC	2	-	6 kg/m	Polyester	Non-linear
	Wave park	2	-	6 kg/m	Polyester	Non-linear
NoviOcean	Single WEC (CFD and LP model)	1	(±75, -8, ±75)	6 kg/m	Polyester	20000 N/m
	Single WEC (LP model)					
	Wave park (LP model)	2	-	6 kg/m	Polyester	Non-linear

Figure 13. Axial load of the polyester mooring varying with relative elongation (Yang et al., 2020b).

2.3 Assumptions and limitations

Assumptions were mainly based on the theory and the modelling approach. The potential theory assumes that sea water is incompressible and inviscid and that fluid motion is irrotational, allowing fluid velocity to be described using a velocity potential (Faltinsen, 1993). The complex Navier-Stokes equation was simplified to the Laplace equation. The limitation is that the potential theory does not consider viscous wave load, which is important in many scenarios. Linear wave theory assumes that the free surface boundary conditions are applied to the mean water level and is valid only when the wave amplitude is small relative to wavelength and body dimension (Faltinsen, 1993).

During the modelling process, the mechanical system of WECs was vastly simplified. For example, the central piston of the NoviOcean concept was simplified as a spring-damper and the value of the PTO damping was simplified as a constant. Those simplifications suit the current study objectives, which are focused on the interaction effects within wave parks.

3 Results

This section summarizes the appended papers I-IV and highlights the main achievements of each and summarizes a selection of essential results. The overall structures and internal connections of the appended papers are illustrated in Figure 14 and Figure 15. The study subject of Papers I-III was the WaveEL concept by Waves4Power. Paper I includes the fundamental comparison of two generations of WaveEL regarding aspects of power output and efficiency. Paper II moves from single WaveEL WEC simulations in Paper I to wave park simulations, assessing the performance of 6-WEC parks and a 10-WEC park under different situations. Paper III is a continuation of Paper II that focuses on the fatigue damage of the mooring lines of one of the 6-WEC wave parks studied in Paper II. It also addresses the influence of mooring line fatigue damages on overall wave park design decisions. Paper IV concentrates on the NoviOcean concept, exploring the CFD method using STAR-CCM+ software, a more accurate but time-consuming model. It also investigates a 2-WEC array with varying WEC distances and wave directions using the LP model.
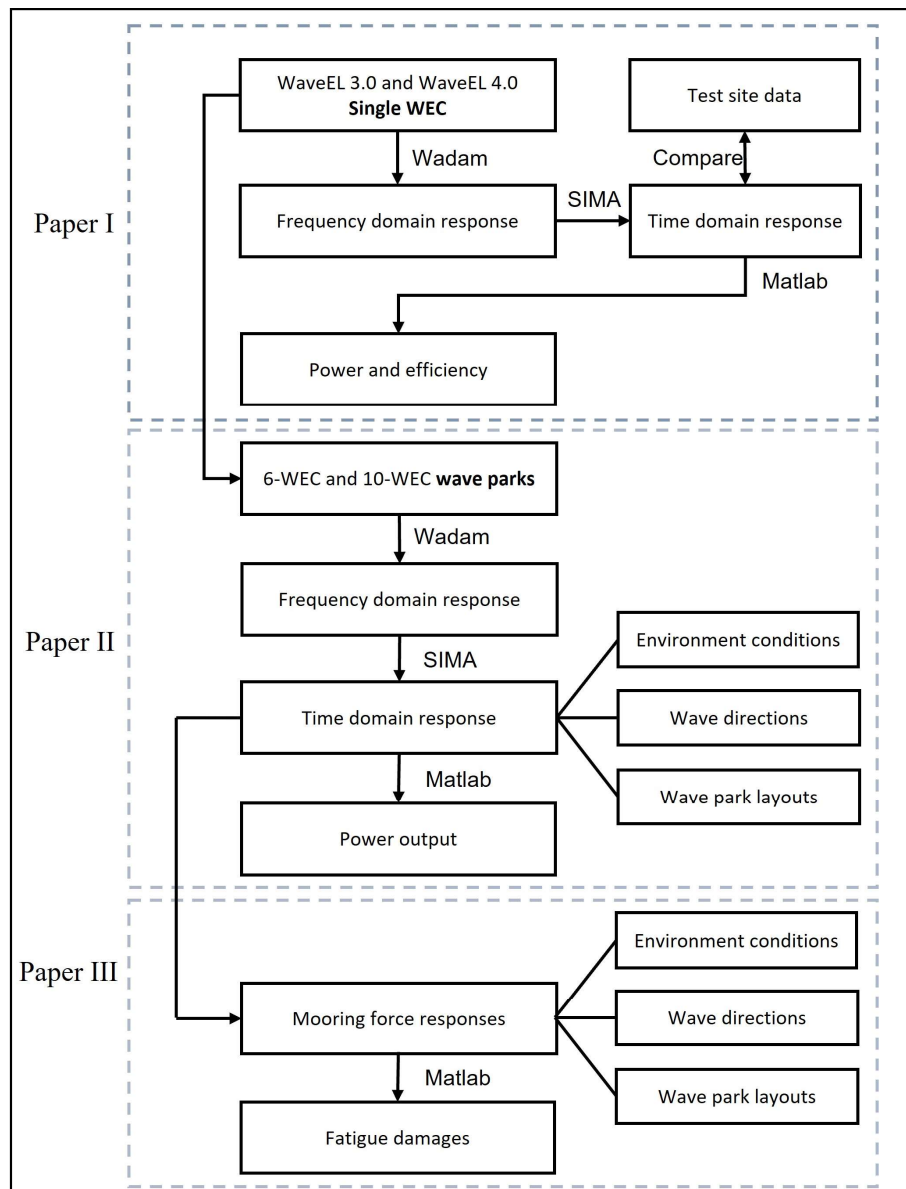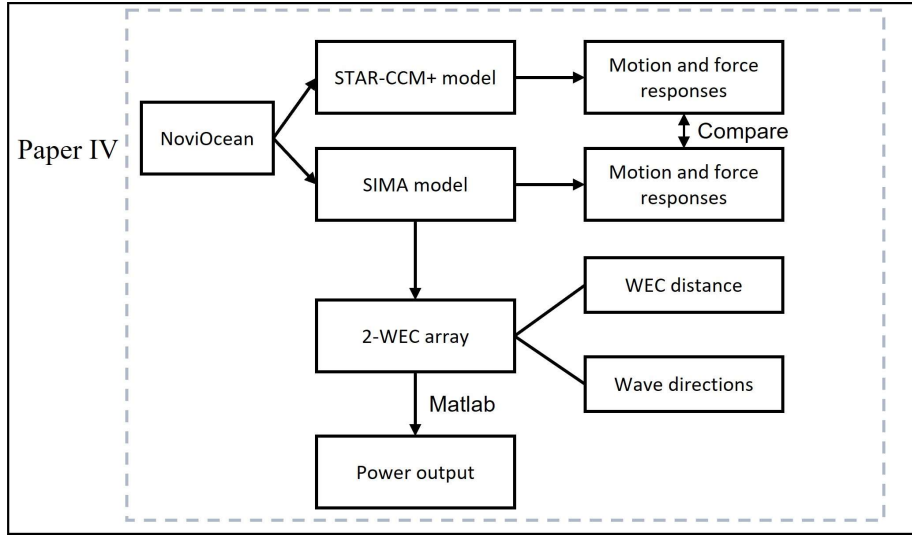

Figure 14. The structures of paper I-III.

Figure 15. The structure of paper IV.

3.1 Summary of Paper I

The purposes of Paper I were to compare the motion responses and power performance of two generations of WaveEL (WaveEL 3.0 and WaveEL 4.0) and validate the WaveEL LP model using experimental data. Validation and comparison of the LP model of the two generations pave the way for wave park evaluations.

The differences between the WaveEL generations are described in Section 2.2.1. The first analysis, carried out in Paper I, was a frequency-domain response analysis, which showed that both generations have a characteristic wave period (resonance) in the frequency domain, with WaveEL 3.0 at 4 s and WaveEL 4.0 at 5 s. WaveEL 4.0 shows a higher heave amplitude response than WaveEL 3.0 at the characteristic wave period (Figure 16). Note that the frequency-domain analysis excluded the mooring system for both generations, as the mooring system introduced in Section 2.2.1 does not add much stiffness to the heave motion.
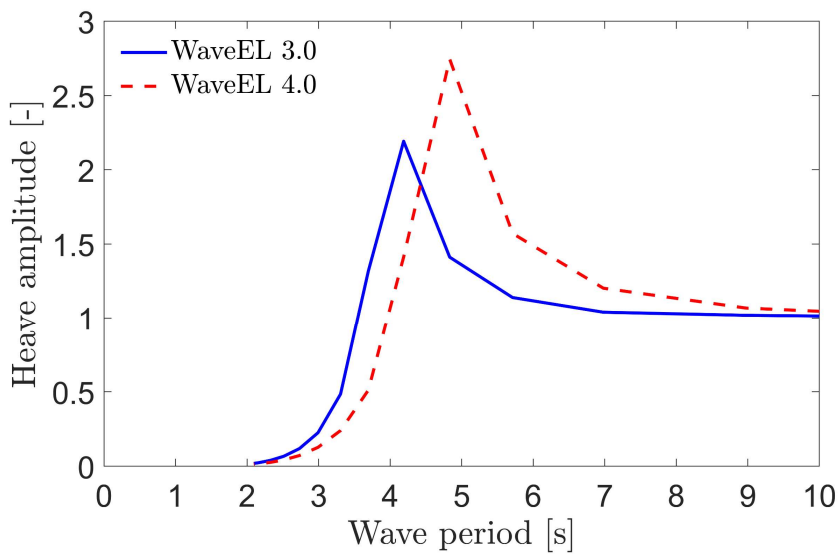

Figure 16. Heave amplitude response per unit wave height with respect to wave periods.

The power output and hydrodynamic efficiency were calculated in the time domain with fully coupled simulations that included the mooring system. A series of regular sea states with wave amplitudes ranging from 0.25 to 3 and wave periods ranging from 2 to 11 were simulated. Figure 17 shows that the largest power output and hydrodynamic efficiency occur at the characteristic wave period, confirming low mooring stiffness distribution in the heave direction. Furthermore, WaveEL 4.0 outperforms WaveEL 3.0 in power output and efficiency at the characteristic wave period.
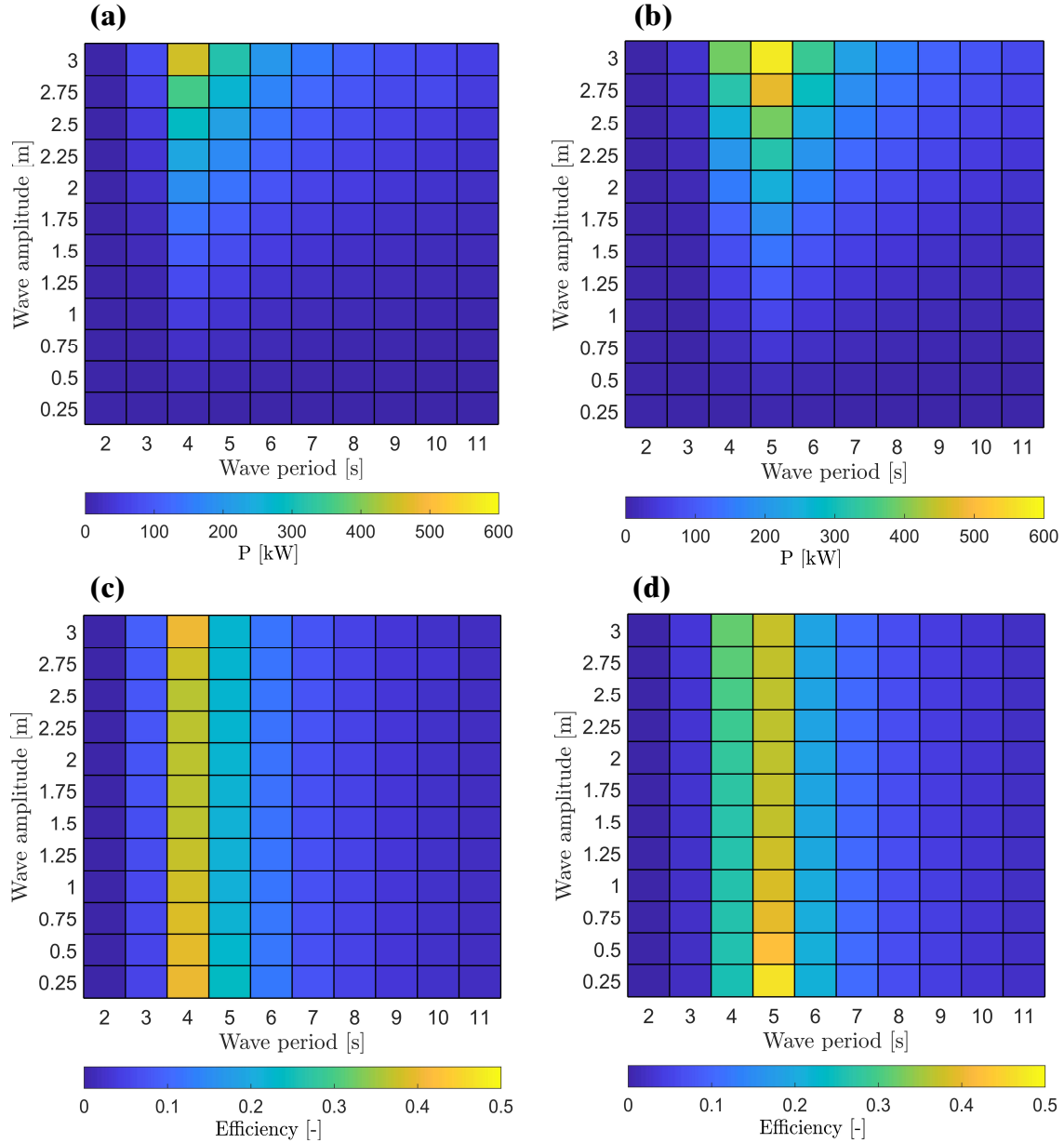

Figure 17. Power outputs and efficiencies of WaveEL 3.0 and 4.0. (a) and (b): power outputs of WaveEL 3.0 and 4.0. (c) and (d): efficiencies of WaveEL 3.0 and WaveEL 4.0.

Figure 18 shows the measured historical buoy position of WaveEL 3.0 during three 2017 Runde test site experiments and the simulated position using identified experimental sea conditions. Overall, the buoy position of WaveEL 3.0 recorded in the experiments overlapped with the envelopes identified in the simulations. In the vertical plane, the range of the heaving motion of simulated WaveEL 3.0 showed good agreement with the

experimental data. However, the measured buoy positions were scattered across larger regions in the water surface plane than in the simulation results of the horizontal plane. As the heave motion is where the power is extracted from, it is confident that the power output calculations based on simulation results are trustworthy. This agreement between the measurement and simulated results of WaveEL 3.0 also validated the simulation model.

The two versions of WECs shared similar ranges of horizontal and vertical buoy position variance under mild sea-state conditions, such as, for example, during the test period on 2017-06-16. WaveEL 4.0 showed significantly larger envelopes in both the horizontal and vertical planes along the incoming wave direction than the former version under environment conditions with large wave heights, such as with the sea-state conditions during the test periods on 2017-06-18 and 2017-06-19.
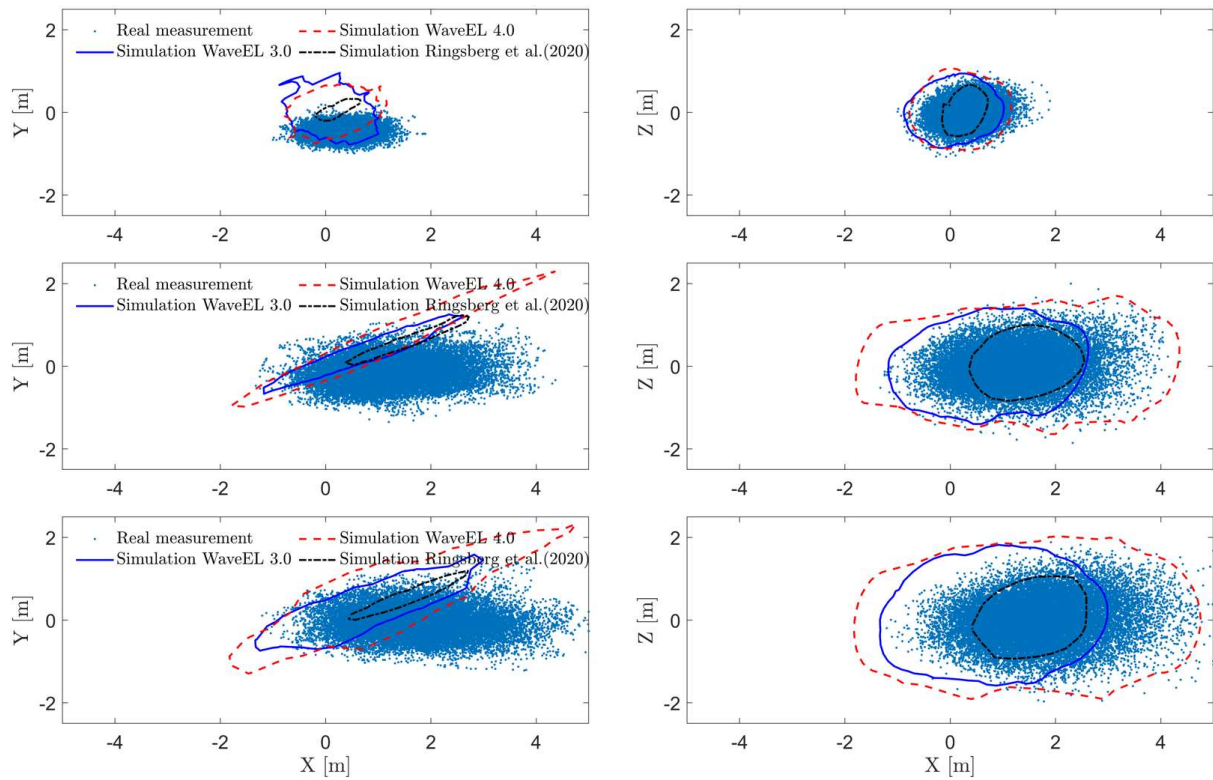

Figure 18. WEC buoy locations at the sea-state condition of 2017-06-16, 2017-06-18 and 2017-06-19 from top to bottom, respectively.

Overall, the newer WaveEL 4.0 generation has a higher heave amplitude and larger resonant period than the previous generation and also shows higher power production performance. However, the disadvantage of the new generation is that it moves on a large region in the horizontal plane. This should be considered in the design of WEC array layouts, where the new generation needs to have a larger distance among the neighbouring units to avoid losing efficiency due to hydrodynamic interaction effects. Nonetheless, considering the increases in the power generation and hydrodynamic efficiency introduced by the geometric modifications of WaveEL 4.0, the extra caution in the array layout design should be deemed worthwhile.

3.2 Summary of Paper II

Paper II evaluated the interaction effects on the power performance of the three wave park layouts shown in Figure 9 under three representative environment conditions (ECs) (Table 9) and several incoming wave directions. EC1 and EC2 were two of the most frequently overserved sea states at the Runde test site from June to November 2017 (Yang et al., 2020a), while EC3 is a relatively harsh sea state. It should be noted that, in Paper II, the effects of wind and current were not considered. Paper II was intended to determine the interconnections between the wave park layouts (shapes and WEC distances), environmental conditions and power performance. This enables recommendations to achieve cost-efficient wave park solutions for different situations.

Table 9. Definition of three ECs selected for detailed study by numerical simulations.

EC	Wave amplitude, A [m]	Wave period, T [s]	Wavelength [m]
EC1	0.25	4.5	31.6
EC2	0.75	5.5	47.2
EC3	1.75	7.5	87.8

Effects of environmental conditions

The normalized power outputs of Hex1-80 wave layout are provided in Figure 19. Note that the hydrodynamic power output of the wave park units for a given environment condition is normalized based on the corresponding power of the single units for the same condition. The performance of most of the units for ECs 1 and 2 for the two generations are enhanced by interaction effects, except for the upstream units at 60º and 300º of WaveEL 4.0. The most efficient unit in all cases is located at 180º, which is the most upstream position. The same result was found by Babarit (2010), which showed that the positive effect of wave interactions is higher for the first WEC encountering the incoming waves than other WECs. Each WaveEL 4.0 in the array performs at least 1.5 times better than that of the single WaveEL 3.0 under the same environment conditions. In contrast to ECs 1 and 2, the power polar maps of both WEC concepts for EC3 almost overlap with that of P_{ref}. This implies that the interaction effects are negligible in extreme environment conditions with large waves. Since the wavelength of EC3 is significantly larger than the WEC buoy diameter, the buoys have limited effects in deflecting, reflecting, and radiating the waves.

Effects of incoming wave directions

The whole array performance is dependent on the wave encounter direction ranging from 150º to 180º due to the symmetric topology of the hexagon shape. The most upstream unit harvests the most power at 180º, while the most downstream two units have the best performance at 150º, as shown in Figure 20. The interaction effects are positive for all wave directions, although they are minor for the upstream units when waves come from 150º. Overall, the performance of the WaveEL 4.0 units is better than WaveEL 3.0. However, the upstream units of WaveEL 4.0 are more affected by the incoming wave directions.

Comparison of 6-WEC arrays

Two wave park layouts (Hex1-120 and Hex2) are compared in Figure 21. Only the performances under EC2 are shown because the interaction effects are not as significant under EC1 and EC3. The wave directions are 150° and 180°, which are aligned with the symmetry axes of the hexagon. In WaveEL 3.0, Hex2 performs slightly better than Hex1-120 under EC2 for the two wave directions. However, in WaveEL 4.0, Hex2 clearly performs worse than Hex1-120 under EC2. The differences in the normalized power between the two wave park layouts are large, which suggests that the interaction effects of WaveEL 4.0 are largely dependent on the layout topology.
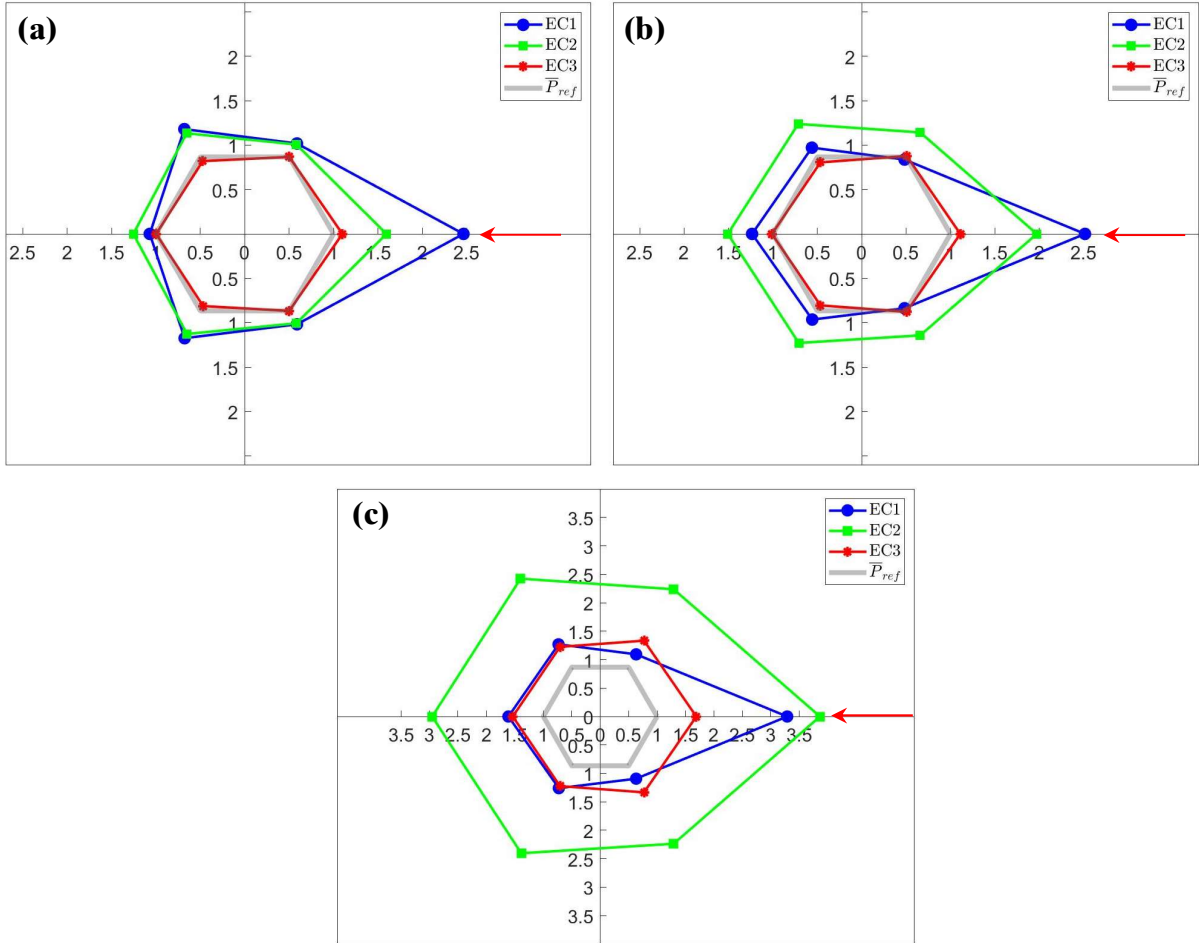

Figure 19. Normalized power output of each WEC unit in the layout sharing the centre anchor with the interval WEC-unit distance of 80 m, Hex1-80, for (a) WaveEL 3.0, (b) WaveEL 4.0, (c) WaveEL 4.0 but normalized with the reference value of WaveEL 3.0. The incoming wave direction is 180°, which is marked with red arrows.
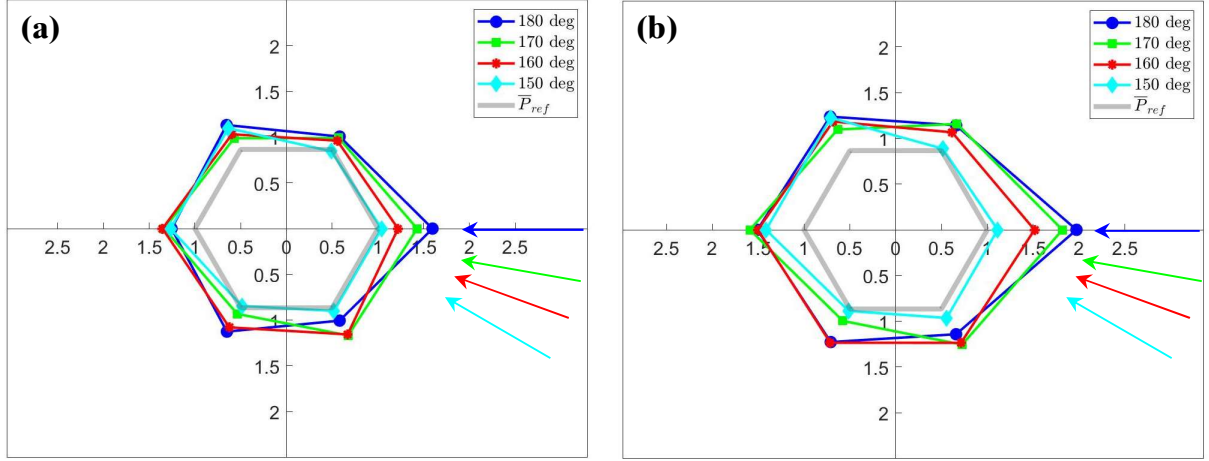
26

Figure 20. Normalized power output from each WEC unit in the array layout Hex1-80 for the environment condition EC2, installed with (a) WaveEL 3.0 and (b) WaveEL 4.0. Arrows indicate wave encounter directions.
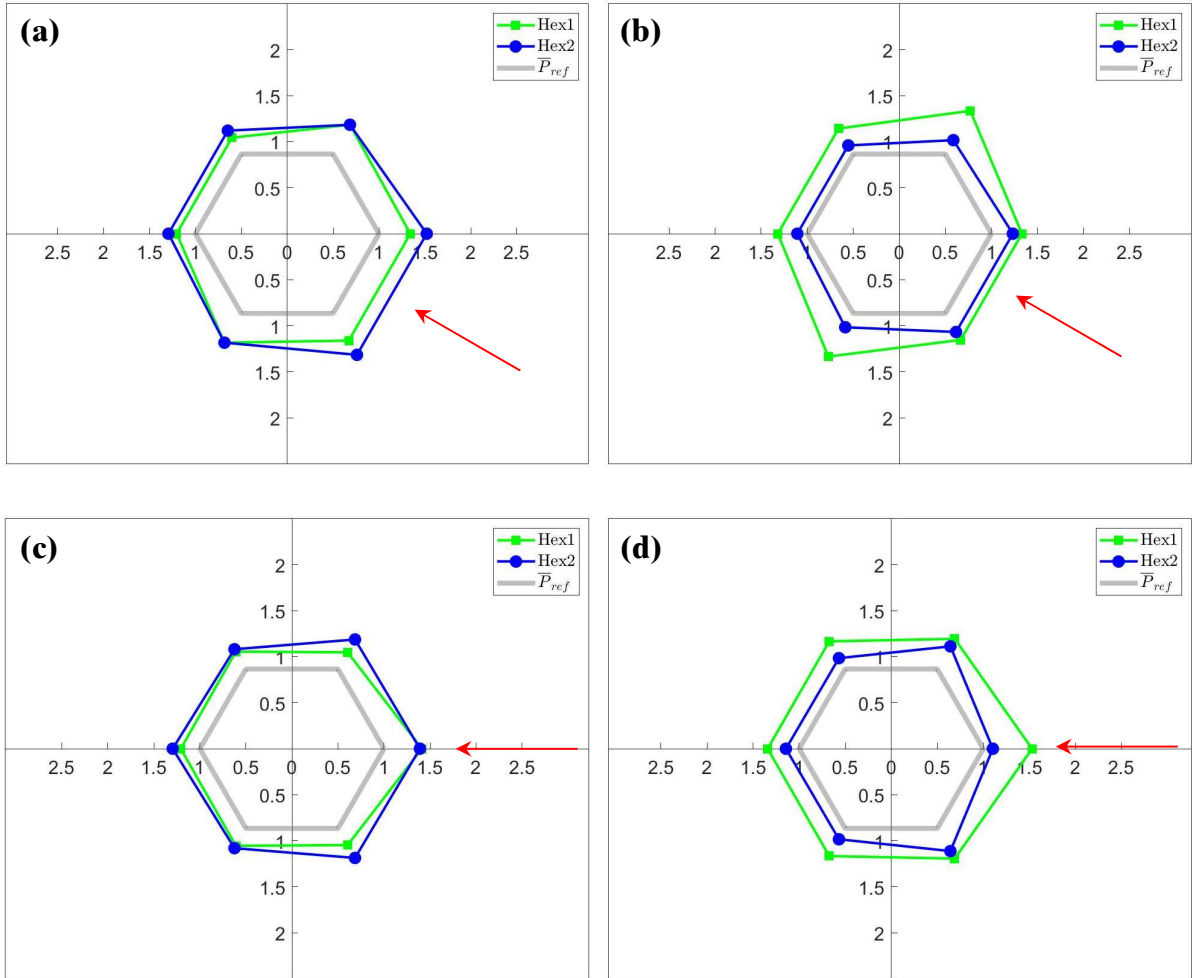

Figure 21. Normalized power generated from the layouts Hex1-120 and Hex2 at EC2 at the wave encounter direction 150o for (a) WaveEL 3.0, (b) WaveEL 4.0, and at 180o for (c) WaveEL 3.0 and (d) WaveEL 4.0. Note that the polar coordinate system is used here, and the unit positions correspond to Figure 9. The red arrows indicate wave encounter directions.

Total power outputs comparison

Figure 22 shows the normalized total power output of the wave parks under three environment conditions, ECs 1–3. In EC1, the Hex2 layout with WaveEL 3.0 outperforms other layouts and WEC types for all wave encounter directions and the total power remains consistent across different wave directions. The same trend is found for this layout in ECs 2 and 3, but the performance improvement is considerably reduced in EC2 and negligible in EC3. This suggests that the interaction effects from the Hex2 and WaveEL 3.0 layout are not significantly affected by the incident wave direction nor environment conditions. EC2 is an ideal environment condition for current WECs and its wavelength is five times the buoy diameter, with a wave frequency comparable to the WEC characteristic frequency. The most efficient layout under EC2 is Hex1-120 installed with WaveEL 4.0. However, its normalized power is reduced by 30% when the wave direction is changed to 150º. In EC3, where there are large and long-period waves, the interaction effects are minimal or slightly detrimental to power absorption. This observation is consistent with previous analyses, as the individual WEC units are nearly decoupled from each other due to the large difference between the wavelength and the WEC dimension. Figure 23 shows the normalized total power output of the entire wave park StarBuoy under EC2 with waves coming from 150-330º. The interaction effects are favourable for StarBuoy, as the minimum performance improvement is around 40%. However, the disadvantage of system is that the total power performance is sensitive to wave direction.
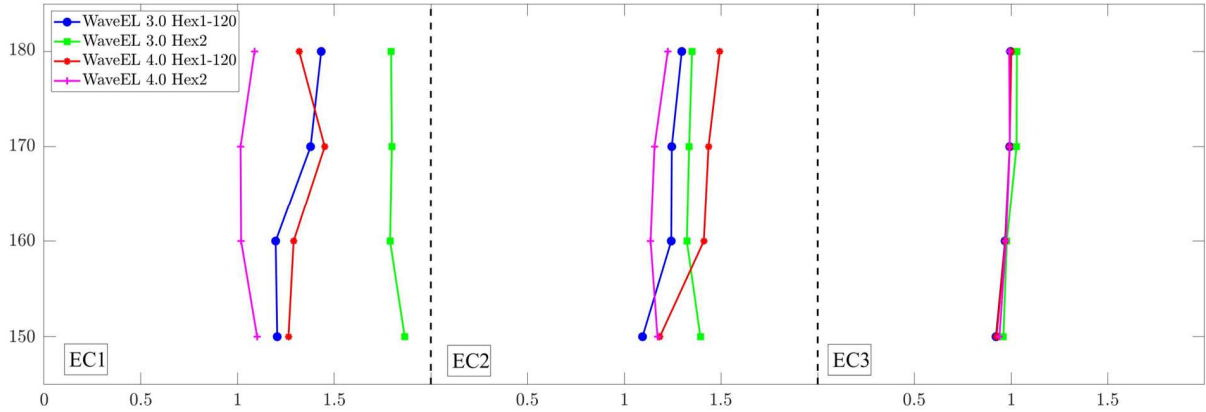

Figure 22. Normalized total power from the entire layouts, Hex1-120 and Hex2, installed with the units of WaveEL 3.0 and 4.0 under the different environment conditions ECs 1-3 and wave incoming direction 150º–180º.

In summary, under EC1 and EC2, the power performance of WaveEL 3.0 and 4.0 in Hex1-80 layout are both enhanced by the interaction effects, and WaveEL 4.0 performs at least 1.5 times better than its counterpart. Under harsh EC3, the power performance of the Hex1-80 wave park is not sensitive to WEC generation or EC. With regard to the incoming wave direction, the wave parks with WaveEL 4.0 shows overall better performance. However, WaveEL 3.0 park shows more stable power output with varying incoming wave directions. With regard to the total power performance of the two wave park layouts, Hex1-120 and Hex2, Hex2 with WaveEL 3.0 performs better than Hex1-120, while Hex2 with WaveEL 4.0 performs worse than Hex1-120 under EC2 with waves coming from 150º and 180º. Overall, these findings shed light on the decision-making

strategy of choosing WEC generation and wave park layout based on wave conditions and directions.
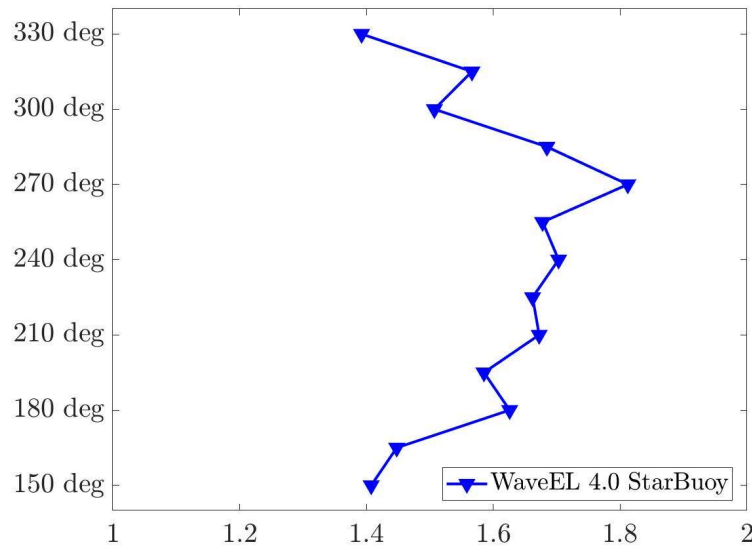

Figure 23. Normalized total power layout of StarBuoy installed with the WaveEL 4.0 unit for wave encounter directions 150º–330º under EC2.

3.3 Summary of Paper III

Paper III is a continuation of Paper II that studied Hex1, one of the three wave park layouts from Paper II, but from the perspective of the accumulated fatigue damage of the polyester mooring lines of the wave park system. This was done because, according the study by Ringsberg et al. (2020a), mooring fatigue life significantly increases the LCOE. Paper III discussed various factors that affect mooring lines' fatigue damage, including environment conditions, WEC versions, incoming wave directions and WEC distances of the wave park. It was intended to provide another perspective on the wave park layout design that considers potential mooring fatigue damage in the overall evaluation of wave park layouts instead of solely considering power performance.

Effects of environment conditions

The effects of environment conditions were studied first. To investigate the effects of environmental conditions, the WEC distance and incoming wave direction were fixed at 80 m and 180° while environment conditions and WEC version were altered. In Figure 24, it can be seen that, under the mild environment condition EC1, the WaveEL 4.0 park accumulates less fatigue damage. However, the WaveEL 3.0 sustains less fatigue damage under the moderate EC2 and the harsh EC3.

Mooring lines were numbered according to a specific convention: the first number following the letter 'M' indicates the WEC number, while the second number stands for the numbering of each mooring. In EC3, the mooring lines belonging to WEC 2, WEC 4, WEC 5, and WEC 6 in the WaveEL 4.0 array accumulate less fatigue damage than their counterparts in the WaveEL 3.0 array (Figure 25). However, the mooring lines of WEC 3 in the WaveEL 4.0 array suffer from more fatigue damage than those of the WaveEL 3.0 array. It is important to note that mooring lines with symmetric locations,

such as M21 and M61, do not accumulate the same amount of fatigue damage due to the harsher sea state in EC3.
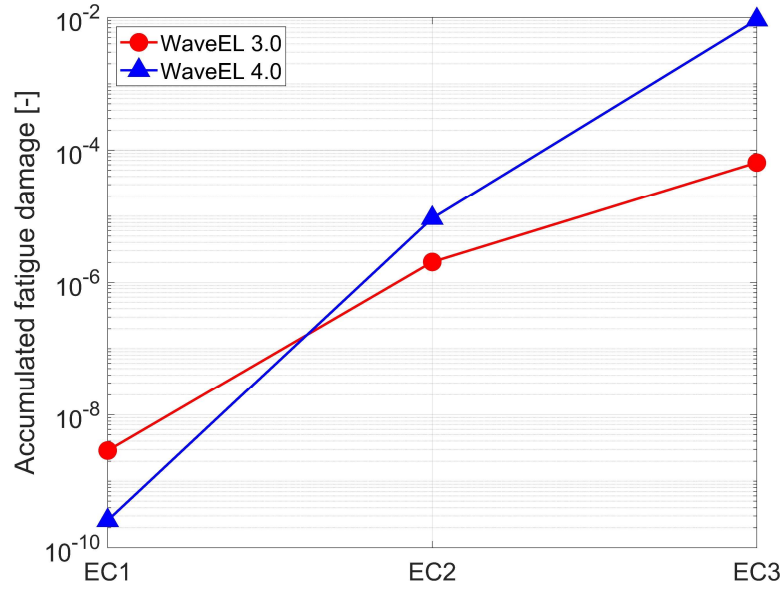

Figure 24. Fatigue life of arrays with different WEC versions and environment conditions.
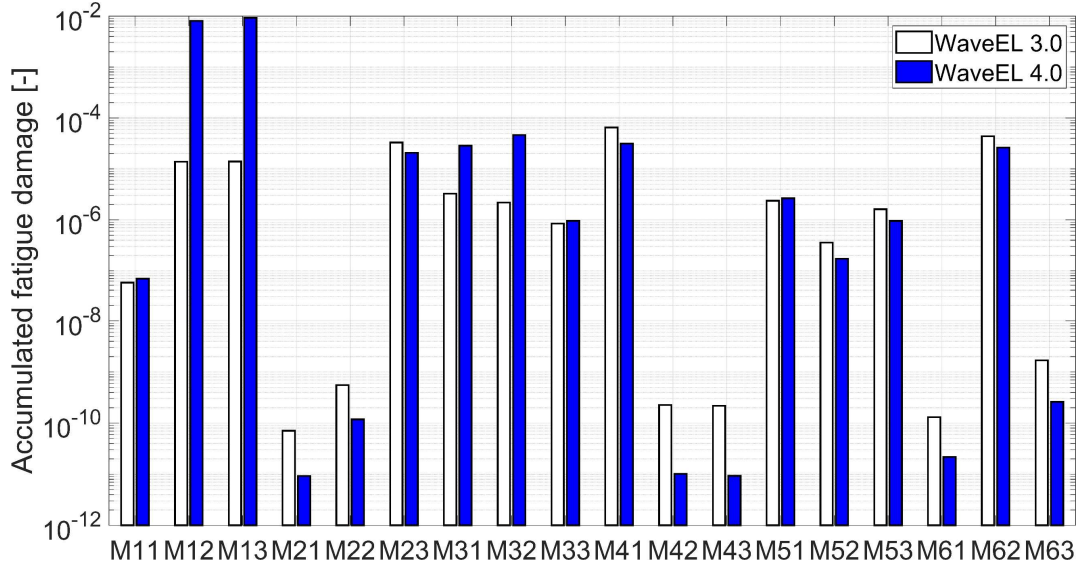

Figure 25. Accumulated fatigue damage in each mooring line for two arrays with two WEC versions under EC3.

Effects of incoming wave directions

The direction of incoming waves affects the accumulation of fatigue damage in mooring lines. Two representative incoming wave directions, 150° and 180°, were chosen to investigate this effect. These directions were selected because they align with two axes of symmetry in the layout. The environment condition used was EC2, which had a high probability of occurrence states at the Runde test site (Yang et al., 2020b). Figure 26 shows the amount of fatigue damage accumulated by each mooring line and the highest accumulated fatigue damage values of each WEC unit. The mooring line that suffers the largest amount of fatigue damage determines the fatigue life of the whole WEC array.

Notably, the two most upstream mooring lines, M12 and M13, suffer the largest amounts of damage for both incoming wave directions. Overall, mooring lines exhibit minor fatigue damage with an incoming wave direction of 180°, with a few exceptions (e.g., M11 and M13).
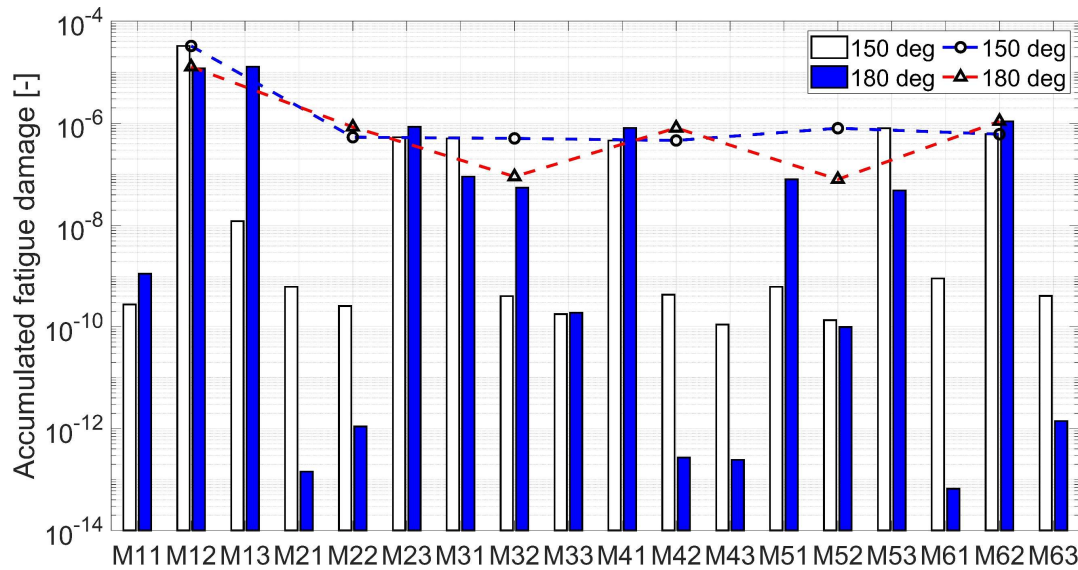

Figure 26. The fatigue life of each mooring line in the WaveEL 4.0 array with incoming wave directions of 150 and 180° under EC2.

Effects of WEC distances

The distances between WECs in a wave park affect both the power output and the fatigue damage of the mooring lines. Figure 27 shows the variation in fatigue damage and power output as the WEC distance changes. The change from WaveEL 3.0 to WaveEL 4.0 causes an increase in power output at all three WEC distances. However, a greater WEC distance does not always result in higher power output. The power output of both parks shows a drop when the WEC distance increases from 80 m to 100 m, followed by an increase when it increases further to 120 m. The fatigue damage decreases, or at least does not increase significantly, when the WEC distance increases. With increasing WEC distance, the WaveEL 4.0 park accumulates less fatigue damage than the WaveEL 3.0 park. At 100 m and 120 m WEC distances, the WaveEL 4.0 park performs better than WaveEL 3.0 from both power and fatigue damage perspectives. However, at an 80 m WEC distance, it is difficult to determine which wave park performs better. This is because, while WaveEL 4.0 has a higher power output, it also accumulates more fatigue damage.
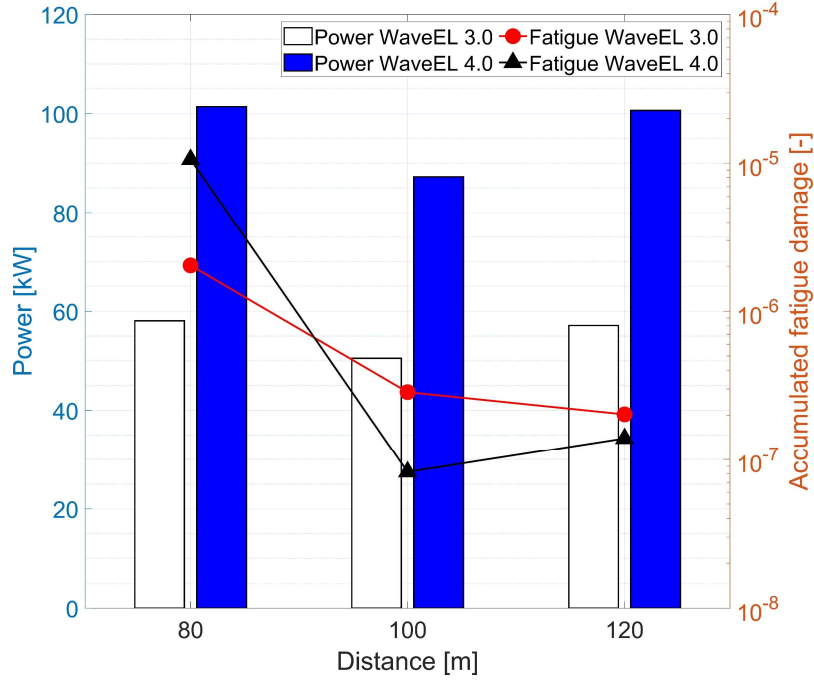
Figure 27. The fatigue life and power output of WEC arrays with different WEC distances.

In summary, the moorings of wave parks with WaveEL 4.0 are prone to suffering larger fatigue damage under harsh environment conditions than WaveEL 3.0. The upstream moorings sustain larger fatigue damage than others and the fatigue damage of mooring lines decreases or remains at a similar level when varying the WEC distance from 80 m to 120 m. However, power performance does not follow the same trend. Rather, it has similar power performance at 80 m and 120 m, but a power drop at a WEC distance of 100 m. This inconsistency necessitates trade-offs when selecting a wave park design. Finally, paper III was not able to predict the fatigue life of mooring lines, as a full scatter diagram with probabilities was not simulated.

3.4 Summary of Paper IV

Paper IV studied the NoviOcean concept with aspects of motion and power performance of a single WEC and a 2-WEC wave park. The aim was to build and verify the non-resonant NoviOcean model with a different geometry and larger dimensions than WaveEL, and analysis the interaction effects within a 2-WEC wave park with different configurations. The NoviOcean concept was simulated using the LP model and CFD model, as explained in Section 2.2.2.

The wave condition simulated was a regular wave with a wave period of 9 s and wave height of 1.8 m, which was suggested by the Novige AB company. Figure 28a shows that both software models provide similar total amplitudes and periods for the heave motion. The CFD model (STAR-CCM+ model in the figures) predicts a heave motion range of -0.56 m to 0.92 m, while the LP model (SIMA model in the figures) predicts a heave motion range of -0.9 m to 0.66 m. Additionally, Figure 28b demonstrates that the total heave force in the LP model is higher than in the CFD model. This difference in heave motion could be explained by the fact that the CFD method considers the transient wetted surface, while the linear potential flow theory does not account for this effect. Rather, the LP model only integrates the hydrodynamic forces on the surfaces below

32

the static mean water level. As a result, the WEC's resistance during its downward motion simulated in LP model was lower, causing the mean value of the heave motion to be higher than that of the CFD method.
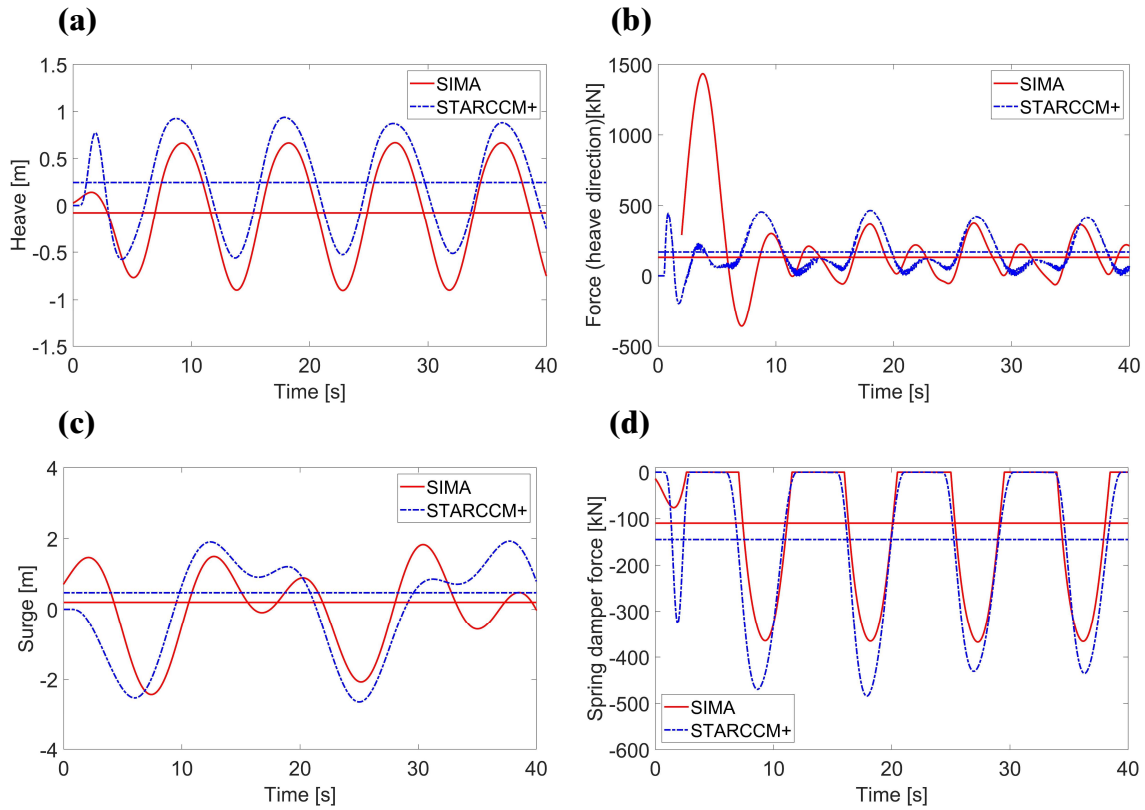

Figure 28. LP (SIMA) and CFD (STAR-CCM+) model comparison: (a) heave, (b) total force, (c) surge and (c) force in central piston. Straight lines indicate the averaged values.

Figure 28c presents a comparison of the surge motions of the buoy of the single unit. It shows slightly different amplitudes between the LP and CFD models, although the changing trends are consistent overall. The forces generated by the central piston, which was represented as a spring-damper system in both software programs, are illustrated in Figure 28d. It should be noted that the spring-damper does not have a repelling force. Although the two models exhibit similar results, the CFD model produces a force that is about 100 kN greater than the LP model. Once again, this disparity is thought to be due to the inclusion of transient wet surface variation in the CFD simulations.

Overall, the LP and CFD models show good agreement within the simulation time regarding heave and surge motion, total force in the heave direction and the force from the central piston. Although the LP model has not been validated by experiments, it was verified by the CFD model. This provides confidence for the 2-WEC wave park analysis using the LP model.
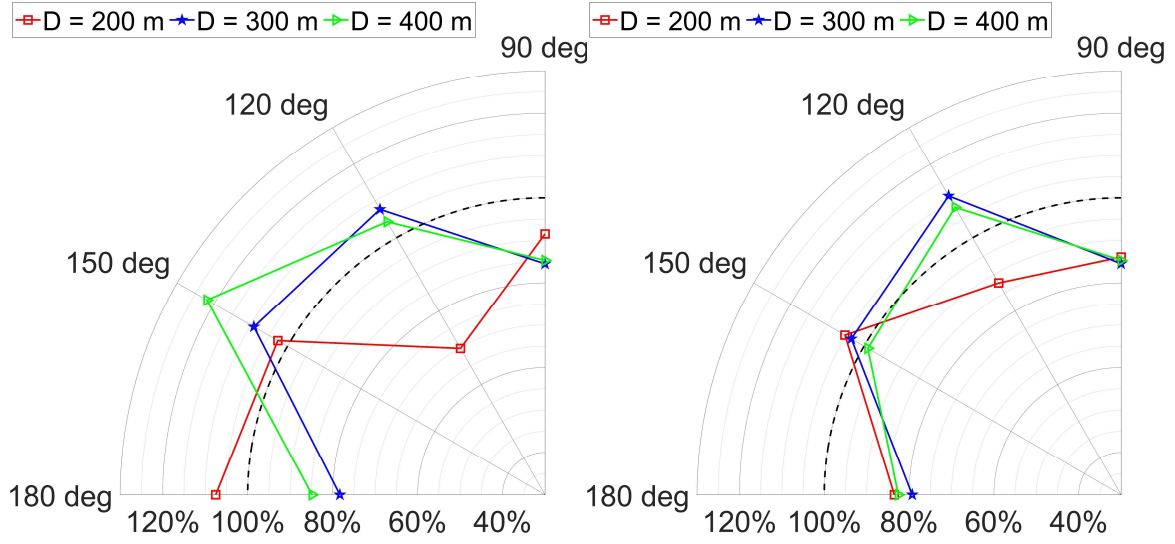
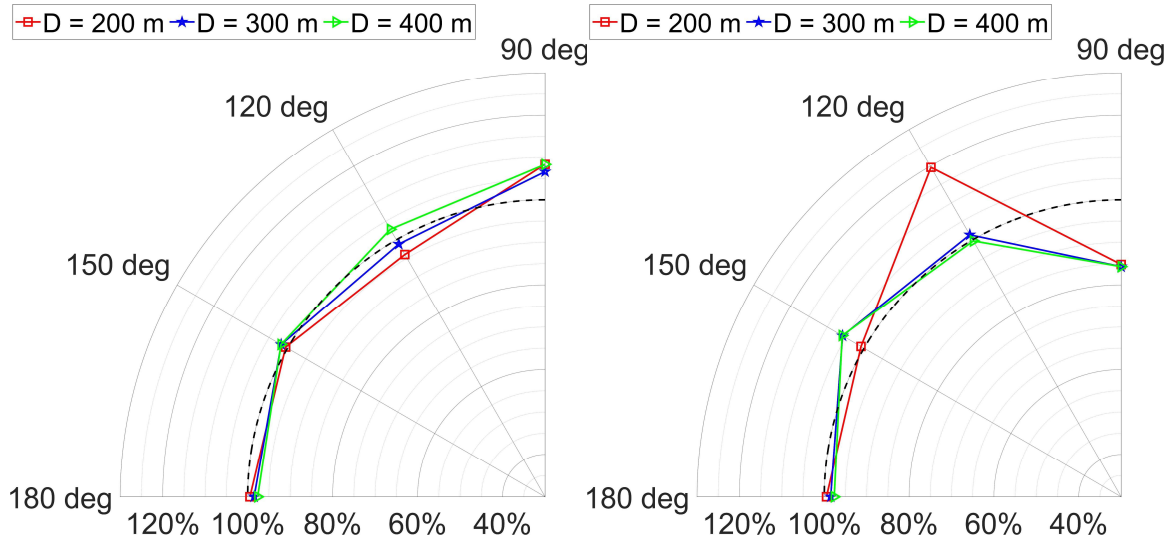Figure 29. The power percentage of Case X: WEC 1 (left) and WEC 2 (right).

Figure 30. The power percentage of Case Y: WEC 1 (left) and WEC 2 (right).

The results of the 2-WEC wave park simulations using LP model are shown in Figure 29 and Figure 30 for the WEC distances of 200, 300 and 400 m. The results indicate the ratio between the power output of a WEC in an array and the power output of the same single-unit WEC under the same environment conditions. The curves show that the power output of the WECs is relevant to the WEC distances and wave directions. However, it is difficult to draw concrete conclusions and recommendations due to the scattered results of each WEC for different WEC distances and wave directions.

In summary, Paper IV verified the LP model with the CFD model regarding motions and forces. It also revealed the importance and complexity of the interaction effects on power performance of wave parks with non-resonant WECs.

4 Conclusions

WECs will have enormous potential in the renewable energy market due to their cost-effective, clean and sustainable features. The design of single WECs and wave parks need careful consideration and multiple tests to guarantee safety and lower costs. This is preferably done by numerical simulations.

The main objective of this thesis is to develop a methodology to cover the modelling, the power output calculation and the mooring fatigue damage evaluation for single WEC and WEC arrays. This has been accomplished by the presentation of the development of two kinds of simulation models, the LP model and CFD model, for single WEC and wave park power performance and mooring fatigue damage estimation. Furthermore, three subgoals of the research (i)-(iii) were defined in Section 1.2. The following paragraphs present in more detail what this thesis concluded in relation to these goals.

(i)   Propose methodologies for different WEC concept to model their characteristics with acceptable accuracy for specific purposes. The methodologies should cover the whole system of single WECs and WEC arrays, including the PTO and mooring systems.

(ii) Investigate the interaction effects of different WEC arrays with different WEC concepts. Evaluate the data systematically concerning the power output performance and the mooring fatigue damage.

(iii) Compare different modelling methodologies and specify their applicable range.

The first simulation model, the LP model, is based on the linear potential theory and the software used was the DNV SESAM software package. This model ignores viscous force and the nonlinear effects, which makes it less accurate under severe sea conditions but with faster computational speed. The second model, the CFD model, is based on the CFD method, and the software used was STAR-CCM+. It is more accurate but requires a large amount of computational power. It was found that, under one selected wave condition, the results of the LP model showed strong agreement with the CFD model in terms of motions and forces. The LP model was hence verified by the CFD model.

The power performance of two generations of WaveEL (WaveEL 3.0 and 4.0) as single WECs was compared and discussed. The WaveEL 3.0 model was validated by experimental data regarding aspects of vertical and horizontal motions. It was found that WaveEL 4.0 has a larger heave response amplitude at the characteristic wave period than WaveEL 3.0 in the frequency-domain analysis. Additionally, it was also demonstrated in the time-domain analysis that WaveEL 4.0 shows higher power performance at the characteristic wave period than WaveEL 3.0. However, it was found that WaveEL 4.0 moves in larger ranges at vertical and horizontal planes than its counterpart under the same environment conditions, which suggests a need for larger distances between WaveEL WECs in wave park designs.

Three wave park layouts with varying WEC distances and WaveEL generations were investigated with aspects of the power performance under different environment conditions and wave incoming directions. It was observed that the power performance

of the Hex1-80 layout with WaveEL 3.0 and 4.0 is improved by interaction effects, and that WaveEL 4.0 performs at least 1.5 times better than its counterpart under mild to moderate environment conditions. Under harsh EC3, the power performance of the Hex1-80 wave park is not sensitive to the WEC generation or the EC. Generally, the wave parks with WaveEL 4.0 have better power performance, while the WaveEL 3.0 park shows more stable power output with varying incoming wave directions. Regarding to the total power performance, Hex2 with WaveEL 3.0 performs better than Hex1-120, while Hex2 with WaveEL 4.0 performs worse than Hex1-120 under EC2, with waves coming from 150° and 180°. The interaction effects are favourable for StarBuoy, with a minimum performance improvement of approximately 40%. However, its total power performance is sensitive to wave direction.

The mooring fatigue damage of the wave park layout Hex1 was also analysed. It was found that the moorings of wave parks with WaveEL 4.0 are more likely to suffer larger fatigue damage under harsh environment conditions than WaveEL 3.0. The upstream moorings sustain larger fatigue damage than others, and it was observed that the fatigue damage of mooring does not share the same variation trend with the power performance when varying the WEC distance. This suggests that there are necessary trade-offs when choosing a wave park design in order to balance the gain of power performance improvements and the loss of mooring line fatigue damage increases.

The NoviOcean concept was investigated by the LP model and CFD model. It was found that, under moderate environment conditions, the two approaches gave similar results, with acceptable differences regarding aspects of heave and surge motions and total forces exerted on the WEC. Two 2-WEC wave parks with different WEC distances and orientations were tested. Although the results showed the correlation between the power output, the WEC distances and orientations, the highly scattered results made it difficult to generate concrete conclusions or recommendations.

5 Future work

The PhD research project aims to develop systematic numerical approaches for single WEC and wave park simulations. This thesis contributed to building, validating and verifying the numerical models for WaveEL and NoviOcean WECs as single WECs and wave parks. Many new conclusions have been reached, as presented in Chapter 4. In this section, some thoughts for future study are categorized and explained.

More factor analysis

The effects of some factors, such as environment conditions, wave incoming directions and WEC distance on the power performance and mooring fatigue damage have been studied thoroughly in this thesis. However, some other factors, such as current, wind, water depth and type of biofouling, are interesting topics for future research. To obtain full mooring line fatigue life predictions, a series of simulations of the full wave scatter diagram is also necessary.

CorPower concept modelling

The CorPower WEC, though not mentioned specifically in this thesis, is also a subject of this overall PhD research. This concept has an innovative wavespring and cascade gearbox inside its buoy, which are unique devices that do not exist in WaveEL and NoviOcean models. These require special simulation models to capture their effects on the WEC motions and, consequently, the power output performance and mooring fatigue damage. The methodology developed thus far may not be applicable to this concept, so a new modelling approach may have to be developed.

More detailed PTO system modelling

The WEC concepts have complex PTO systems. The current two models cannot model complex contact, shaft and gear components within the PTO systems. These were simplified in the current models as linear dampers. However, it is unclear whether these simplified systems greatly impact the power output estimation. In the future, new software such as Ansys (Ansys, 2023) and WEC-sim (WEC-sim, 2023) should probably be used to enable more detailed modelling of the PTO systems.

Control algorithms in PTO system

Applying controlling methods to the PTO system, such as latching and adjusting of PTO damping according to the simultaneous incoming wave, is an effective way to increase power output performance. In wave parks, incoming waves are altered by multiple WECs. Therefore, controlling each PTO system may be even more critical to reduce the negative interaction effects and boost total power output performance. However, controlling is not considered in the current single WEC and wave parks models. The previously mentioned new approaches, Ansys and WEC-sim, could provide more flexibility in including control algorithms.

6 References

Alves M. (2016) Frequency-Domain Models. *Numerical Modelling of Wave Energy Converters.* Elsevier, 11-30.

Ansys. (2023) *Ansys*. Available at: https://www.ansys.com/.

Babarit A. (2010) Impact of long separating distances on the energy production of two interacting wave energy converters. *Ocean Engineering* 37: 718-729.

Babarit A. (2013) On the park effect in arrays of oscillating wave energy converters. *Renewable Energy* 58: 68-78.

Balitsky P, Verao Fernandez G, Stratigaki V, et al. (2017) Assessing the Impact on Power Production of WEC array separation distance in a wave farm using one-way coupling of a BEM solver and a wave propagation model. *EWTEC2017.* 1176-1186.

Budal K. (1977) Theory for Absorption of Wave Power by a System of Interacting Bodies. *Journal of Ship Research* 21: 248-254.

Clément A, McCullen P, Falcão A, et al. (2002) Wave energy in Europe: current status and perspectives. *Renewable and Sustainable Energy Reviews* 6: 405-431.

Devolder B, Stratigaki V, Troch P, et al. (2018) CFD Simulations of Floating Point Absorber Wave Energy Converter Arrays Subjected to Regular Waves. *Energies* 11.

DNV. (2021) Offshore standards position mooring

Downing SD and Socie DF. (1982) Simple rainflow counting algorithms. *International Journal of Fatigue* 4: 31-40.

Falcão AFdO. (2010) Wave energy utilization: A review of the technologies. *Renewable and Sustainable Energy Reviews* 14: 899-918.

Falnes J. (1980) Radiation impedance matrix and optimum power absorption for interacting oscillators in surface waves. *Applied Ocean Research* 2: 75-80.

Falnes J. (2007) A review of wave-energy extraction. *Marine Structures* 20: 185-201.

Faltinsen O. (1993) *Sea loads on ships and offshore structures*: Cambridge university press.

González-Longatt F, Wall P and Terzija V. (2012) Wake effect in wind farm performance: Steady-state and dynamic behavior. *Renewable Energy* 39: 329-338.

Jin S and Greaves D. (2021) Wave energy in the UK: Status review and future perspectives. *Renewable and Sustainable Energy Reviews* 143: 110932.

Krivtsov V and Linfoot B. (2014) Basin Testing of Wave Energy Converters in Trondheim: Investigation of Mooring Loads and Implications for Wider Research. *Journal of Marine Science and Engineering* 2: 326-335.

Lee H, Poguluri S and Bae Y. (2018) Performance Analysis of Multiple Wave Energy Converters Placed on a Floating Platform in the Frequency Domain. *Energies* 11: 406.

Li X, Xiao Q, Zhou Y, et al. (2022) Coupled CFD-MBD numerical modeling of a mechanically coupled WEC array. *Ocean Engineering* 256: 111541.

LiVecchi A, Copping A, Jenne D, et al. (2019) Powering the blue economy; exploring opportunities for marine renewable energy in maritime markets. *US Department of Energy, Office of Energy Efficiency and Renewable Energy. Washington, DC* 207.

Mingham C, Qian L and Causon D. (2016) Computational Fluid Dynamics (CFD) Models. *Numerical Modelling of Wave Energy Converters.* 105-122.

Novige. (2023a) *LIFE Project*. Available at: https://noviocean.energy/life-project/.

Novige. (2023b) *NoviOcean concept*. Available at: https://noviocean.energy/concept-general-innovation-marine-blue-energy-non-resonant-buoyant/.

Poguluri SK, Kim D and Bae YH. (2021) Hydrodynamic Analysis of a Multibody Wave Energy Converter in Regular Waves. *Processes* 9: 1233.

Polinder H and Scuotto M. (2005) Wave energy converters and their impact on power systems. *2005 International conference on future power systems.* IEEE, 9 pp.-9.

RIFLEX. (2019) RIFLEX 4.16.2 Theory Manual.

Ringsberg JW, Jansson H, Örgård M, et al. (2020a) Design of Mooring Solutions and Array Systems for Point Absorbing Wave Energy Devices—Methodology and Application. *Journal of Offshore Mechanics and Arctic Engineering* 142.

Ringsberg JW, Yang S-H, Lang X, et al. (2020b) Mooring forces in a floating point-absorbing WEC system – a comparison between full-scale measurements and numerical simulations. *Ships and Offshore Structures* 15: S70-S81.

Runge C. (1895) Ueber die numerische Auflösung von Differentialgleichungen. *Mathematische Annalen* 46: 167-178.

SIMA. (2023) *SIMA Documentation.* Available at: https://www.sima.sintef.no/doc/4.4.0/sima/index.html.

SIMO. (2019) SIMO 4.16.2 Theory Manual.

Stallard T, Stansby PK and Williamson AJ. (2008) An experimental study of closely spaced point absorber arrays. *The Eighteenth International Offshore and Polar Engineering Conference.* OnePetro.

STAR-CCM+. (2023) *Simcenter STAR-CCM+ - Engineer innovation with multiphysics computational fluid dynamics (CFD) simulation.* Available at: https://www.plm.automation.siemens.com/global/en/products/simcenter/STAR-CCM.html.

Stensvold T. (2017) *Norge har fått sitt første bølgekraftverk som leverer strøm til kraftnettet. Slik virker det.* Available at: https://www.tu.no/artikler/norge-har-fatt-sitt-forste-bolgekraftverk-som-leverer-strom-til-kraftnettet-slik-virker-det/395569.

Ubbink O. (1997) Numerical prediction of two fluid systems with sharp interfaces.

Wadam. (2017) SESAM user manual Wadam.

Wadam. (2023) *Frequency domain hydrodynamic analysis of stationary vessels - Wadam.* Available at: https://www.dnv.com/services/frequency-domain-hydrodynamic-analysis-of-stationary-vessels-wadam-2412.

Waves4Power. (2021) The WaveEL-System - A Technical Description. 8.

WEC-sim. (2023) *WEC-sim v5.0.1*. Available at: https://wec-sim.github.io/WEC-Sim/master/index.html.

Weller S, Stallard T and Stansby P. (2010) Experimental measurements of irregular wave interaction factors in closely spaced arrays. *IET Renewable Power Generation* 4: 628-637.

Yang S-H. (2018) Analysis of the fatigue characteristics of mooring lines and power cables for floating wave energy converters. *Department of Mechanics and Martime Sciences.* Chalmers University of Technology, 114.

Yang S-H, Ringsberg JW and Johnson E. (2017a) Parametric study of the dynamic motions and mechanical characteristics of power cables for wave energy converters. *Journal of Marine Science and Technology* 23: 10-29.

Yang S-H, Ringsberg JW and Johnson E. (2020a) Wave energy converters in array configurations—Influence of interaction effects on the power performance and fatigue of mooring lines. *Ocean Engineering* 211: 107294.

Yang S-H, Ringsberg JW, Johnson E, et al. (2017b) Biofouling on mooring lines and power cables used in wave energy converter systems—Analysis of fatigue life and energy performance. *Applied Ocean Research* 65: 166-177.

Yang S-H, Ringsberg JW, Johnson E, et al. (2020b) Experimental and numerical investigation of a taut-moored wave energy converter: a validation of simulated mooring line forces. *Ships and Offshore Structures* 15: S55-S69.

Yang S-H, Ringsberg JW, Johnson E, et al. (2018) Experimental and numerical investigation of a taut-moored wave energy converter: A validation of simulated buoy motions. *Proceedings of the Institution of Mechanical Engineers, Part M: Journal of Engineering for the Maritime Environment* 232: 97-115.

Yang S-H, Ringsberg JW, Johnson E, et al. (2016) A comparison of coupled and de-coupled simulation procedures for the fatigue analysis of wave energy converter mooring lines. *Ocean Engineering* 117: 332-345.